The American Journal of Human Genetics, Volume *108*

Supplemental Data

SCUBE3 loss-of-function causes a recognizable recessive developmental disorder due to defective bone morphogenetic protein signaling

Yuh-Charn Lin, Marcello Niceta, Valentina Muto, Barbara Vona, Alistair T. Pagnamenta, Reza Maroofian, Christian Beetz, Hermine van Duyvenvoorde, Maria Lisa Dentici, Peter Lauffer, Sadeq Vallian, Andrea Ciolfi, Simone Pizzi, Peter Bauer, Nana-Maria Grüning, Emanuele Bellacchio, Andrea Del Fattore, Stefania Petrini, Ranad Shaheen, Dov Tiosano, Rana Halloun, Ben Pode-Shakked, Hatice Mutlu Albayrak, Emregül Işık, Jan M. Wit, Marcus Dittrich, Bruna L. Freire, Debora R. Bertola, Alexander A.L. Jorge, Ortal Barel, Ataf H. Sabir, Amal M.J. Al Tenaiji, Sulaima M. Taji, Nouriya Al-Sannaa, Hind Al-Abdulwahed, Maria Cristina Digilio, Melita Irving, Yair Anikster, Gandham S.L. Bhavani, Katta M. Girisha, Genomics England Research Consortium, Thomas Haaf, Jenny C. Taylor, Bruno Dallapiccola, Fowzan S. Alkuraya, Ruey-Bing Yang, and Marco Tartaglia

Supplemental Note: Case Reports

Family 1 (Italy)

Sib 1 **(F1S1)** is a female of 19 years old. She is the first child from consanguineous parents without a history of relevant disorders. Cesarean delivery occurred at 40th week of gestation after an unremarkable pregnancy. Birth weight was 3,020 g (-0.9 SDS), length 46 cm (-2.2 SDS) and occipitofrontal circumference (OFC) 33 cm (-1.1 SDS). Apgar score was 8 and 9 at 1 and 5 minutes, respectively. At birth, short stature and craniofacial dysmorphisms were observed while ultrasound investigations excluded other internal organ defects. Psychomotor development was normal. X-ray analyses at 14 years disclosed growth delay, abnormality of cervical bones (hypoplastic odontoid process), increased distance of the dorsal intervertebral space, and irregularly shaped lumbar vertebral bodies. Oligodontia, abnormality of shape of the residual teeth, dental crowding and malocclusion were also documented. At the last evaluation (19 years), bone age was at least 2 years less than chronologic age, according to Greulich-Pyle; height was 135.4 cm (-4.7 SDS), OFC 54 cm (-0.5 SDS), weight 43.1 kg (-2.3 SDS) and BMI 23.5 (0.6 SDS). She had craniofacial dysmorphisms including a long oval face with high forehead, hypotelorism, blepharoptosis, and a high nasal bridge, piriform nose with bulbous tip, enlarged naris, pointed chin and thick vermilion, and micrognathia. Joint laxity was also observed. Further X-ray analyses confirmed epistrophy hypoplasia, scoliosis with left-convex deviation, and squared lumbar vertebral bodies. Skull bones were normally shaped. Notably, all epiphyses including the metacarpal heads were reduced in length. Further findings included camptodactyly and narrow iliac wings. Dental abnormalities, including agenesis of all molar teeth except mesial molar and dental crowding, were unchanged. Cardiological, abdominal and routine laboratory investigations, also including testing for metabolic disorders, were unremarkable.

Sib 2 **(F1S2)** is a 10-year-old female, second child of the same consanguineous parents. Cesarean delivery occurred at 35 weeks of gestation after an uncomplicated pregnancy. A previous spontaneous miscarriage was recorded. Birth weight was 2,390 g (0.1 SDS), length 43 cm (-1.2 SDS) and OFC 33 cm (0.8 SDS). Apgar score was 9 and 10 at 1 and 5 minutes, respectively. Similar to her older sister, short stature and craniofacial dysmorphisms were observed at birth. Cranial and abdominal US scan were normal; dysmorphisms included triangular face with high forehead, hypotelorism, blepharoptosis, high nasal bridge, piriform nose, pointed chin, thick vermilion and micrognathia. A subcutaneous cleft palate was also seen, and surgically corrected at 5 months. There was no developmental delay nor intellectual disability. At 7 years, X-ray analyses showed vertebral defects (squared lumbar vertebral bodies), limbs defects (reduced thickness of the distal epiphysis of the radius and proximal epiphysis of the tibia), and hip dysplasia (coxa valga with cervico-diaphyseal angle 150°, asymmetry of femoral heads with flattened medial part). At the last evaluation at 10 years, height was 102.6 cm (-5.8 SDS), OFC 53 cm (-1.0 SDS), weight 14.8 kg (-6.0 SDS), and BMI 13.9 (-1.8 SDS). Previously identified defects of vertebral, iliac and limbs bones were confirmed. Dental abnormalities including multiple agenesis of permanent teeth, dental crowding, and multiple caries were also documented. Cardiological, abdominal, laboratory and metabolic investigation were unremarkable.

For both sibs, chromosome and high-resolution CGH-array (180K) analyses excluded the presence of clinically relevant CNVs. Based on their complex phenotype, both sibs were enrolled in the Undiagnosed Patients Program at the Ospedale Pediatrico Bambino Gesù for further molecular

investigations. Collection, use and storage of clinical data, pictures, and biological material of the patients and their parents were attained after written informed consent was secured.

Family 2 (India)

Sib1 **(F2S1)**, a 22-year-old male born to first cousin parents, presented with short stature. He had a history of seizures from 1 to 5 years of age. Hearing loss due to eardrum problems was documented, though records were not available for review. He had myopia of the right eye from 15 years of age. On examination (22 years), his height and weight were 151.5 cm (-3.6 SDS) and 60.5 kg (-1.3 SDS), respectively. He had a long triangular face, high forehead, hypotelorism, blepharoptosis, high nasal bridge, bulbous nose, enlarged nares, prominent ear pinna, deep set eyes, high arched palate, crowded teeth and pointed chin. Cafe-au-lait spots, hypopigmented macules on the abdomen and transverse striae on the back were also observed.

His younger 15-year-old brother **(F2S2)** also presented with short stature. His height and weight were 147 cm (-2.5 SDS) and 39.4 kg (-2.0 SDS), respectively. He reported a single episode of seizures at 1 year of age. Hearing impairment was also documented, which was corrected by adenoid surgery. On examination, he had similar dysmorphic features as his elder brother.

Both probands had cutaneous syndactyly and hallux valgus. Intellectual development was normal for both of them. On radiological survey, thin phalanges, mild scoliosis and squared lumbar vertebral bodies, narrow iliac wings, and coxa valga were observed in both siblings.

Family 3 (Iran)

The proband **(F3S1)** is a female who is presently 39 years old. She is one of five children born to consanguineous parents. Her parents and unaffected sister have a history of miscarriage. Apart from a male cousin who reports the same syndrome, there are no other disorders that have been reported in their distant family. She was born in the 38th gestational week with a birth weight of 1,400 g (-5.8 SDS) and length of 33 cm (-9.2 SDS). Due to lack of prenatal care, there were no concerns about these aspects mentioned in her medical history. She is currently 132 cm (-3.5 SDS) with an OFC of 52 cm (-2.2 SDS). She has a long triangular face, high forehead, hypotelorism, a piriform nose with high nasal bridge and a deviated septum. Mild large ears and dental crowding have been documented. Sonography of the kidney, uterus, and ovaries was unremarkable. X-ray analysis documented narrow iliac wings and acetabular dysplasia. She has elementary education and is not reported to have intellectual disability.

Her 29-year-old sister **(F3S2)** was born in the 38^{th} gestational week after an unremarkable pregnancy and delivery. She is currently 130 cm (-3.8 SDS). She showed craniofacial dysmorphisms including a long triangular face with high forehead, high nasal bridge, and piriform nose.

The third sib **(F3S3)** is a 25-year-old male. He was born in the 38^{th} gestational week after an unremarkable pregnancy and delivery. He currently has a height of 144 cm (-3.5 SDS), a sitting height of 121 cm, waist height of 87 cm, and arm span of 145 cm. He has a BMI of 19.8 (-1.3 SDS). He has several craniofacial dysmorphic features including a long triangular face, high forehead, hypotelorism, high nasal bridge with a deviated septum and a down-pointed nose. Dental abnormalities that include

oligodontia and severe dental crowding were documented. He has narrow iliac wings. X-ray studies are not available. He has a mild hearing loss. No other abnormalities are noted.

Family 4 (Sri Lanka)

The proband **(F4S1)** is an 11.5-year-old male, the first child of normal statured first cousin Sri Lankan parents without a family history of relevant disorders. An antenatal scan at 20 weeks showed reduced growth although the pregnancy was otherwise unremarkable. He was born in good condition at 37 weeks via normal vaginal delivery, weighing 1,590 g (-4.6 SDS), with a length of 41cm (-4.6 SDS) and an OFC of 35 cm (0.1 SDS). He was admitted to the special care unit for 3-4 weeks to establish feeding and required nasogastric tube feeding due to poor sucking. He presented to the genetics team just before 2 years of age due to severe short stature and microcephaly. He crawled at 8 months, walked at 13 months but only spoke 4-5 words aged 2 years. His speech and language were markedly delayed relative to his other milestones. Social interaction was limited, with rigid behaviors and difficulty making friends. Subsequent skeletal survey suggested narrow iliac wings, coxa valga, bowing of long bones, mesomelia (upper limbs more pronounced than lower limbs) and bilateral congenital radial head dislocations (felt to be congenital). Consultation of a gastroenterologist for failure to thrive and restricted intake did not identify any medical cause. Endoscopy (aged 8 years) revealed microscopic mild esophageal eosinophilia. Constipation was recorded in childhood but improved with age. Dental anomalies included large lateral incisors, ectopic permanent teeth, bilateral taurodontism in first permanent molars, multiple dental caries (poor oral hygiene), enamel hypoplasia, and dental overcrowding.

At last evaluation (10.5 years), height was 107.3 cm (-3.4 SDS), OFC 48 cm (-4.4 SDS) and weight 13.7 kg (-5.2 SDS). On examination reduced elbow extension, supination and pronation were noted. He had a triangular facies, very small maxilla and mandible, a beaked nose and a high-pitched voice. His hands, feet and ears impressed as large in childhood. Joint laxity and mild fifth finger clinodactyly were documented. (Table 1, Figure 1 and Table S1). He had two younger brothers, neither of whom had similar clinical features. He was recruited to the 100,000 genome project along with his parents and younger brother. Collection, use and storage of clinical data, photographs, biological materials of the patient and parents were obtained after informed verbal consent was secured.

Family 5 (Turkey)

Sib 1 **(F5S1)** is a male referred for short stature at the age of 11.6 years. He was born as the first out of five children from consanguineous healthy but short parents. After an uneventful pregnancy and delivery at 40 weeks of gestation he was born small for gestational age (birth weight 2,500 g, -2.4 SDS). Birth length and head circumference (OFC) were not measured. Besides severe growth failure, the patient had a history of frequent viral infections of the upper respiratory tract. Early motor development was normal (walking at 1.5 years), but school performance has been poor. At physical examination (11.6 years), height was 123 cm (-3.3 SDS), sitting height/height ratio 0.512 (-0.2 SDS), OFC 47.5 cm (-4.6 SDS), weight 21 kg (-4.1 SDS), and BMI 13.9 (-2.3 SDS). He showed craniofacial dysmorphisms including a long triangular face with high forehead, high nasal bridge, piriform nose with bulbous tip, pointed chin and full lips. There was also severe caries and gingival recession. X-ray analyses at 12.5 years disclosed increased lumbar lordosis, scoliosis, and coxa valga. Skeletal age was

10.5 years at a chronological age of 11.6 years. Cardiological and routine laboratory investigations were unremarkable. Serum IGF-I and IGFBP-3 were within the reference range and the GH peak after clonidine provocation was also normal (17 ng/ml).

Sib 2 **(F5S2)** is a female referred for short stature at 7.3 years of age. She is the third out of five children of these consanguineous parents. The three other siblings are healthy and of normal stature. After an uneventful pregnancy she was born after 36 weeks of gestation with a weight of 2,500 g (-0.2 SDS). Birth length and OFC were not measured. Besides severe growth failure, the patient had a history of frequent viral infections of the upper respiratory tract. Psychomotor development was normal. At physical examination (7.3 years), height was 102 cm (-4.2 SDS), sitting height/height ratio 0.553 (1.3 SDS), OFC 48 cm (-3.9 SDS), weight 14.0 kg (-4.0 SDS) and BMI 13.5 (-1.6 SDS). She showed craniofacial dysmorphisms as observed in her brother, including a long triangular face with high forehead, high nasal bridge, piriform nose with bulbous tip, pointed chin and full lips. There was also severe caries and gingival recession. Cubitus valgus was noticed as well. Skeletal age was 7.1 years at a chronological age of 8.1 years. At 8.1 years, X-ray analyses showed scoliosis. A cardiac rhythm disorder (ventricular extrasystoles accompanying first degree AV block) was observed. Routine laboratory investigations were unremarkable. Serum IGF-I and IGFBP-3 were within the reference range and the GH peak after clonidine provocation was also normal (9.4 ng/ml).

For both sibs, the presence of clinically relevant CNVs was excluded by chromosome analysis [SNP array analysis (CytoScan HD array, Affymetrix) in case 1, karyotyping in case 2]. Based on their complex phenotype, both sibs were enrolled in the Genetics in Growth research program at the Leiden University Medical Center for further molecular investigations. Collection, use and storage of clinical data, pictures, biological material of the patients and their parents were obtained after written informed consent was secured.

Family 6 (Saudi Arabia)

The proband is a 16 month-old baby girl **(F6S1)** who was born at term to a healthy second cousin Saudi Arab couple by a normal vaginal delivery. Pregnancy was complicated by an abnormal prenatal ultrasound at 5 months detecting short extremities with intrauterine fetal growth retardation. At birth, weight was 2,500 kg (-2.3 SDS), length 45.5 cm (-2.4 SDS) and OFC 31.5 cm (-2.5 SDS). Apgar scores were 3 and 6 at 1and 5 minutes, respectively. She required chest compression with intubation and ventilatory support and weaned off to CPAP and then to a nasal cannula. She was noticed to have short limbs, hypotonia and distinct facial features (frontal bossing, depressed nasal bridge, anteverted broad nostrils, flat face, midfacial hypoplasia, posteriorly angulated auricles) and joints stiffness. She had feeding difficulties requiring parenteral nutrition followed by nasogastric tube feeding. The initial echocardiogram showed an atrial septal defect (ASD) with pulmonary hypertension. At follow up (16 months), an intact septum was observed. Skeletal X-rays at 14 months showed abnormal cervical vertebra without other bone abnormalities. At 16 months of age, the child had achieved a normal social and motor development for age. Growth parameters showed a height of 65 cm (-4.9 SDS), OFC 42 cm (-2.8 SDS) and weight of 7 kg (-2.9 SDS). The head showed frontal bossing, bilateral epicanthal folds, depressed nasal bridge, broad nostrils, flat face round face, posteriorly angulated auricles with prominent antihelix, dental abnormalities (malalignment of the lower incisors), and small chin. Extremities showed flat feet with eversion. Array CGH showed excessive homozygosity with a normal

copy number. Metabolic investigations (serum ammonia, lactic acids, plasma acylcarnitines and long chain fatty acids) were normal.

Family 7 (United Arab Emirates)

A 25-month old male infant of Yemeni origin **(F7S1)** was first born to healthy first cousin parents. Mother had regular antenatal follow up with no issues apart from an antenatal scan that showed a mild fluid collection around one of the testicles of the fetus. He was delivered by vacuum-assisted vaginal delivery at term. He was flat at birth with meconium-containing liquor and Apgar scores of 1 and 3 at 1 and 5 minutes, respectively. He required immediate respiratory support but had a difficult intubation due to severe micro-retrognathia, glossoptosis and an anteriorly placed airway, resembling Pierre Robin Sequence. His birth weight was 2,900 g (-1.5 SDS), and OFC at birth was 35.5cm (-0.5 SDS). The earliest measured length was 48 cm at 7 weeks (-2.9 SDS). He subsequently underwent a tracheostomy at 2 months of age. He displayed multiple facial dysmorphic features including frontal bossing, hypertelorism, bilateral strabismus, flat nasal bridge, enlarged nares, cleft palate, low set ears, down slanting palpebral fissures and claw shaped right hand with syndactyly. He had a patent foramen ovale that subsequently had closed at follow up echocardiograms. He exhibited oropharyngeal dysphagia and severe gastroesophageal reflux disease that necessitated gastrostomy tube feeding. Additionally, he had tracheobronchomalacia, hypospadias and cryptorchidism and has had repair of lateral ventral hernia. He had severe growth failure, generalized hypotonia and global developmental delay.

He currently requires nocturnal oxygen support. Because the multiple congenital malformations, he was highly suspected to have a genetic syndrome. Chromosomal microarray did not reveal any pathogenic copy number variants.

Family 8 (Brazil)

The proband **(F8S1)** is a 12.8-year-old boy, the second child of consanguineous, first-degree relatives. His older brother does not present congenital anomalies. During pregnancy, intrauterine growth restriction and oligohydramnios were noted. He was born at 37 weeks, by cesarean section, with a birth weight of 2,315 g (-2.8 SDS), length of 41cm (-4.6 SDS), OFC of 34 cm (-0.8 SDS) and Apgar scores 8/8 at 1/5 minutes. He presented with respiratory distress, requiring mechanical ventilation. Pierre-Robin sequence and bilateral premature closure of the coronal suture were diagnosed at that time. Surgical correction of the craniosynostosis was performed at 3 months of age, followed by mandibular distraction osteogenesis. He required gastrostomy for feeding difficulties from 3 to 15 months of age. Complementary exams disclosed patent foramen ovale and pulmonary hypertension on echocardiogram and normal abdominal ultrasound, audiologic evaluation and G-banded karyotype. He was released from hospital after 6 months. Surgical correction of the palatal anomaly was performed at the age of 4 years. He had normal motor development, but presented difficulty in speech. He presented with recurrent otitis. Audiologic evaluation disclosed conductive hearing loss, requiring hearing aids.

He was first evaluated in our institution at the age of 25 months, showing a weight of 8.2 kg (-3.5 SDS), length of 71cm (-4.3 SDS), OFC of 46.7cm (-1.6 SDS); dysmorphic facial features with brachycephaly, high forehead, arched eyebrows, hypoplastic supraorbital ridges, hypertelorism,

bulbous tip of the nose, small mouth, bifid uvula, microretrognathia, prominent ears, and limited elbow extension.

He attends regular school, with no history of learning problems. Because of short stature, endocrinologic assessment was carried out at the age of 5 years disclosing normal plasma levels of IGF1 and a normal GH response to a GH-stimulation test. Complementary exams showed a normal cranial and temporal CT-scan, ophthalmologic evaluation, echocardiogram and chromosomal breakage study with diepoxybutane. Brainstem evoked response audiometry with mild conductive hearing loss and skeletal survey showed mild hypoplasia of the proximal radius; posterior arch defect in cervico-thoracic region; trapezium-1st metacarpal and cuneiform/cuboid-metatarsal coalitions, with broad phalanges.

Patient initiated treatment with recombinant human growth hormone (rhGH 50 μg/kg/d) at the age of 10.6 years due to severe short stature: height of 116.3 cm (-3.9 SDS), sitting height of 63.9 cm {sitting height/total height SDS of 2.6), weight 19.9 kg (-4.0 SDS), BMI of 14.7 kg/m^2 (-1.4 SDS) and OFC 50.5 cm (-2.1 SDS). Physical examination at the last visit at the age of 13.2 years showed a height of 131.0 cm (-3.4 SDS), sitting height of 71.6 cm (SH/H SDS of 3.5), OFC 51 cm (-2.6 SDS), weight 30.0kg (-3.2 SDS), BMI of 17.5 kg/m^2 (-0.5 SDS) and patient is still on treatment with rhGH. Skeletal survey of the patient at 12.8 years documented spine defects (mild lumbar scoliosis, partial fusion of C5-C6 and failure of the posterior arch fusion in C7-T1), and several long bones abnormalities including generalized flattened epiphysis, bowed radius with abnormal radial head at the elbow joint, hypoplastic styloid processes of the ulna and radius and the tibia and fibula. Hands and feet bone defects included trapezoid-2nd metacarpal coalition in both hands and cuneiform bones-2nd and 3rd metatarsals coalitions, as well as cuboid-4th metatarsal coalition in the feet.

Family 9 (Israel)

Patient **F9S1** is an 8 year-old male, the fourth child born to consanguineous reportedly healthy parents of Arab-Muslim descent. Prenatal follow-up was notable for ultrasound findings of left hydronephrosis and short long bones. Amniocentesis was not performed. He was born via vaginal delivery at 42 weeks of gestation, birth weight was 4,050 g (+1.1 SDS) and OFC 36.5 cm (+1.7 SDS). He was hospitalized for the first 51 days of life due to respiratory problems and failure to gain weight. Renal ultrasound at 4 weeks (and again at 6 weeks of age) showed mild hydronephrosis of the left kidney and minimal pyelectasis of the right kidney. Brain ultrasounds, as well as a total-body radiograph (at 3 weeks) were considered normal, even though large cardiothymic silhouette and bilateral hyperinflation were noticed at chest radiographs. Echocardiogram was normal. At ophthalmic investigation, he was reported to have unexplained nystagmus. MRI of the brain and orbits (at 5.5 years) was considered normal. His development and cognitive status were reportedly normal. Due to short stature, he underwent growth hormone stimulation test that was normal. Total body radiological investigation documented shortened proximal limbs, relatively short 1st metacarpal, fusion of the proximal and middle phalanges of the fifth toe in both feet. The bones of the hand also had a coarse appearance. Inborn errors of metabolism (urine organic acids and acylcarnitine) were ruled out. Chromosomal microarray analysis was considered normal, and showed multiple areas of homozygosity. Physical examination (at 8 years and 1 month) was notable for a peculiar facial appearance, with a long, sparse hair, oval face, a pyriform, pear-shaped nose with bulbous tip and large ears. He also had dental crowding and his front teeth had a saw-like appearance. He showed

pectus excavatum and limited flexion of his fingers and hand grip difficulties. In his last visit, at the age of 8 years and 10 months, his weight was 21.3 kg (-2.0 SDS), height was 116.2 cm (-2.8 SDS), and OFC was 51 cm (-1.15 SDS).

Patient **F9S2** is a 22.5 year-old female, the maternal cousin of Patient F9S1. She is the second of three daughters, born to consanguineous reportedly healthy parents of Arab-Muslim descent. The pregnancy was uneventful, and amniocentesis was not performed. She was born via vaginal delivery at 39 weeks of gestation, birth weight was 3,080 g (-0.8 SDS). At infancy she was breastfed but had showed failure to thrive, for which she was hospitalized and evaluated. Echocardiogram showed ostium secundum ASD, which later resolved itself. As her cousin (F9S1), horizontal nystagmus in both eyes was noticed from as early as the first months of life, for which she underwent Kestenbaum procedure. Visual evoked potential (VEP) and electroretinography (ERG) were considered normal. During the first year of life, she had respiratory illnesses and was diagnosed with unilateral congenital lobar emphysema (of the left upper lobe). Brain CT, EEG and metabolic screening were considered normal. Craniofacial dysmorphisms at 5 years included short, brittle and sparse hair whisker hair and sparse both eyebrows and eyelashes maxillary hypoplasia, pointed chin, hypodontia with agenesis of several lower incisors, dental crowding, and short stature. Radiograph of the left hand at 11.5 years was consistent with a bone age of 10 years, and karyotype was 46,XX. Despite her development and cognitive status were reported to be normal, she was considered to show some behavioral issues in early childhood, and underwent assessments for ADHD, learning difficulties and speech delay. However, she attended at school regularly. At 12.5 years, she showed a long face, bright curly hair, high forehead attached earlobes with a protruding antitragus, downslanting palpebral fissures, anteverted nares and a columella below ala nasi, long pointed and triangular chin, irregular teeth with agenesis of several lower teeth, several cutaneous telangiectasias, hallux valgus of both feet with short first and fifth toes. Her weight was 30.4 kg (-1.9 SDS), height was 137.2 cm (-2.1 SDS), and OFC was 51.5 cm (-2.3 SDS). Upon last evaluation (at 22.5 years) her weight is 44 kg (3rd centile) and her height is 146 cm (-3.1 SDS).

Patient **F9S3** is the maternal aunt of F9S1 and F9S2. She is currently 54 years old, and reported to have short stature (145 cm) and clinical features resembling those observed in her nephew and niece, such as an inability to properly form a fist. She is reported to be cognitively normal. Unfortunately, she was unavailable for in-depth phenotyping.

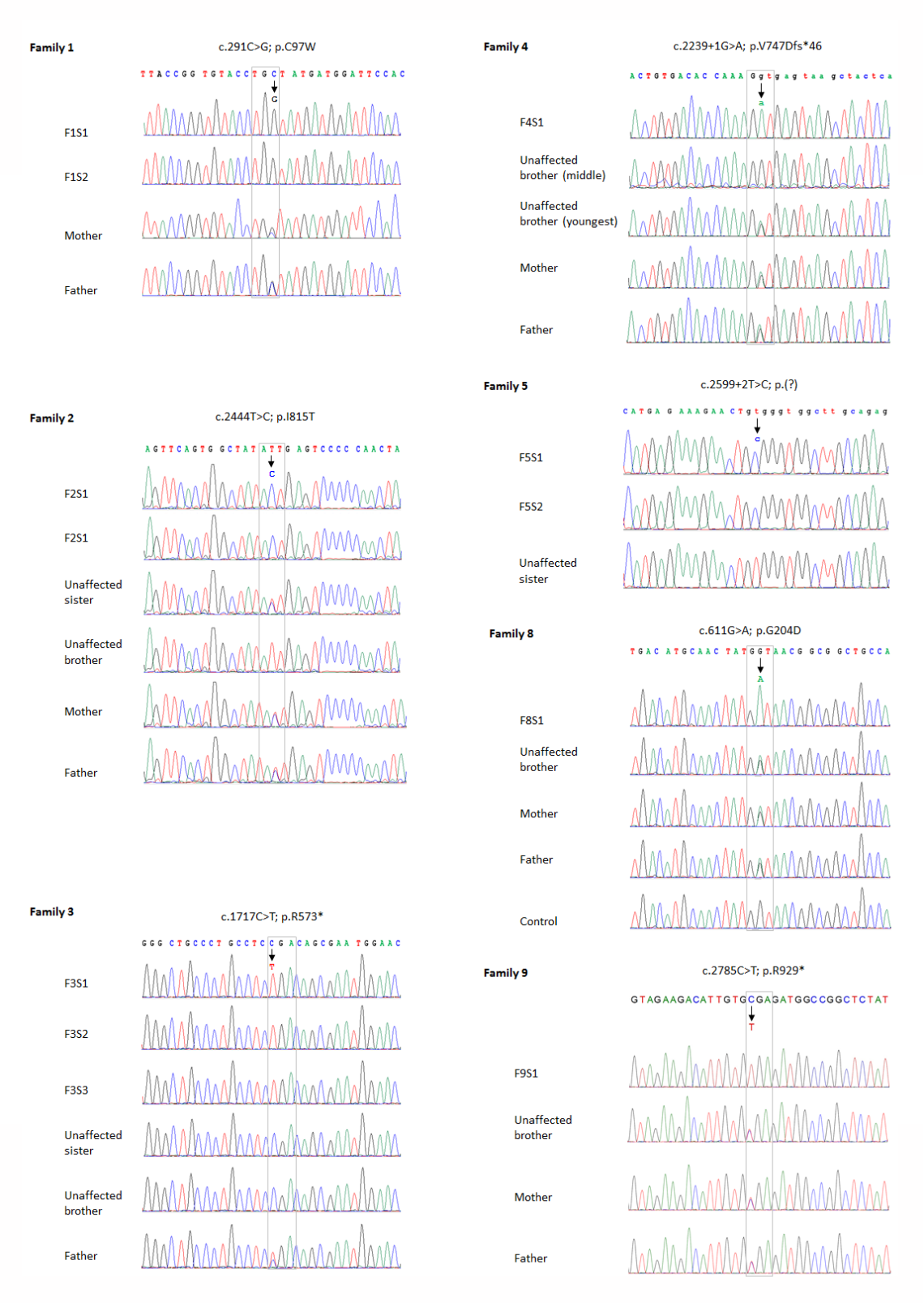

Figure S1. Sanger validation and segregation analyses.
Sequence chromatograms showing homozygosity for the pathogenic *SCUBE3* variants identified in affected members of families 1, 2, 3, 4, 5, 8 and 9.

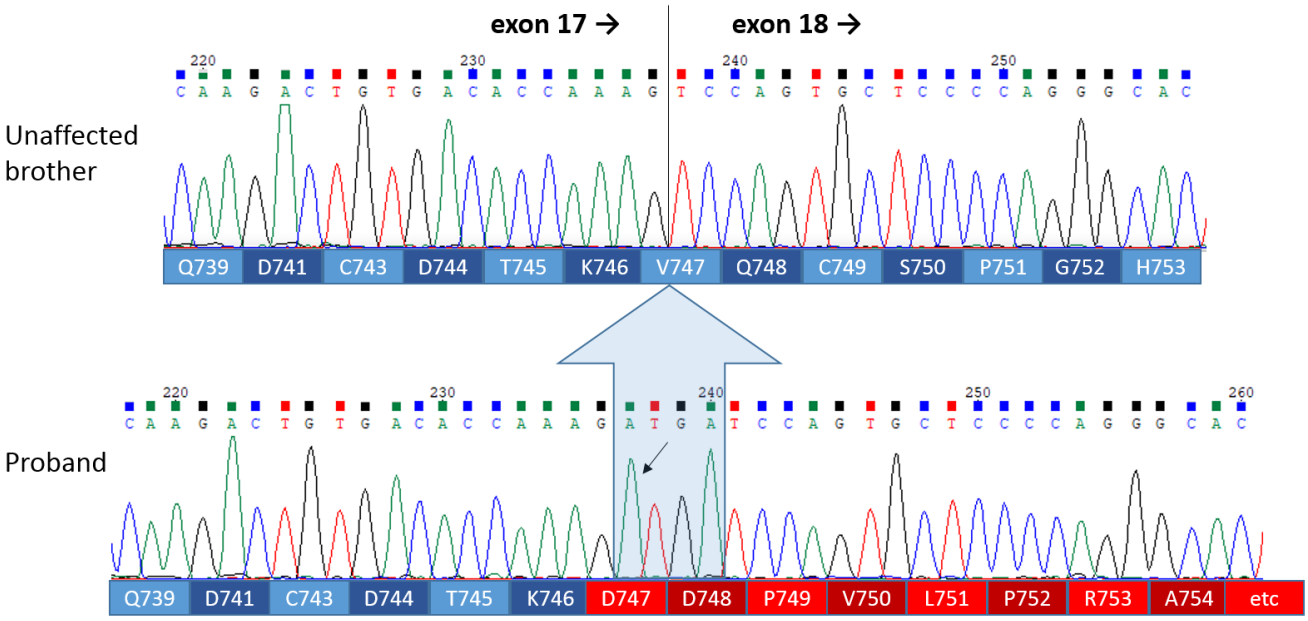

Figure S2. Functional impact of the c.2239+1G>A splice site change (family 4).
Total RNA was used to amplify the relevant cDNA region (exons 17 and 18). Sanger sequencing demonstrates that the c.2239+1G>A variant (black arrow) in *SCUBE3* (NM_152753.2) results in retention of 4 bp of the flanking intronic sequence (blue arrow), predicting an out-of-frame stretch of 45 residues followed by a stop codon (p.Val747Aspfs*46).

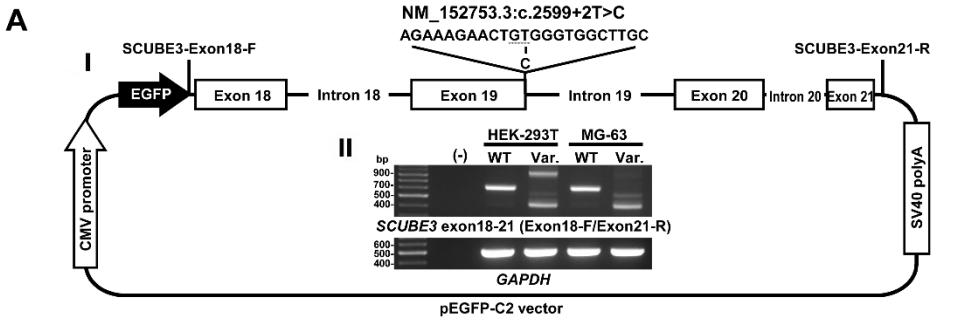

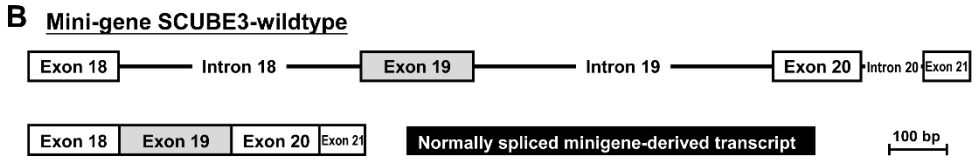

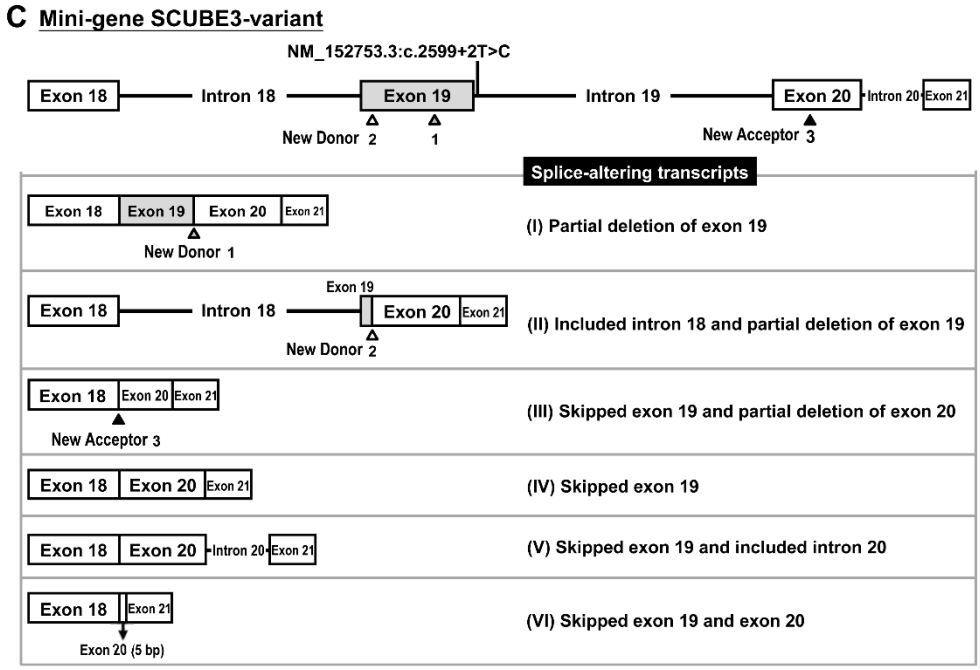

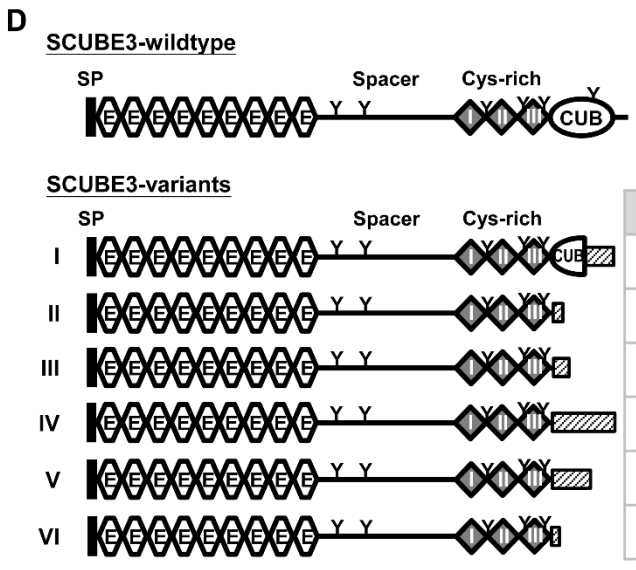

Amino Acid Change	%
p.(Val846Hisfs*57)	4
p.(Asn801Serfs*20)	17
p.(Asn801Argfs*32)	25
p.(Asn801Thrfs*127)	33
p.(Asn801Thrfs*78)	17
p.(Asn801Metfs*8)	4

Figure S3. Mini-gene splicing analysis of the *SCUBE3* c.2599+2T>C variant.

(A) Construction of the splicing vector pEGFP-C2 containing the wild-type (WT) or mutant *SCUBE3* mini-gene. The location of c.2599+2T>C variant (Var.) in the assay is indicated. (I) Straight lines indicate the forward and reverse primers used for RT-PCR. (II) Agarose gel electrophoresis for RT-PCR products. *SCUBE3* Exon18-F and *SCUBE3*-Exon21-R primers were used for RT-PCR amplification of cDNA sequences generated by HEK-293T or MG-63 (an osteosarcoma cell line) cells transfected with each mini-gene. RT-PCR analysis revealed aberrant transcripts produced by the *SCUBE3* mini-gene containing the c.2599+2T>C variant compared to the wild-type *SCUBE3* minigene. *GAPDH* was used as positive RT-PCR control.

(B) The wild-type *SCUBE3* mini-gene contains four exons (open boxes) and 3 functional introns (lines) (upper panel). Normally spliced transcript that excludes intron sequence is depicted (lower panel).

(C) The *SCUBE3* mini-gene contains four exons (open boxes) and 3 introns (lines) (upper panel) and has the disease-associated variant, c.2599+2T>C, which is located in the donor splice site of intron 19. Six splice-altering transcripts were identified in transfected HEK-293T (I to V) or MG-63 cells (II to VI) characterized by: (I) partial deletion of exon 19 (new donor site, gray triangle); (II) inclusion of intron 18 and partial deletion of exon 19 (new donor site, open triangle); (III) skipping of exon 19 and partial deletion of exon 20 (new acceptor site, black triangle); (IV) skipping exon 19; (V) skipping exon 19 and inclusion of intron 20; (VI) skipping of exon 19 and exon 20.

(D) The wild-type *SCUBE3* transcript encodes a polypeptide of 993 amino acids, whereas these splice-altering transcripts result in different out-of-frame products having premature stop codons. Clone frequency (%) for each transcript is shown (n=20). SP, signal peptide; E, EGF-like repeats; Cys-rich, cysteine-rich motifs; CUB, the CUB domain. Y marks potential N-linked glycosylatabled sites.

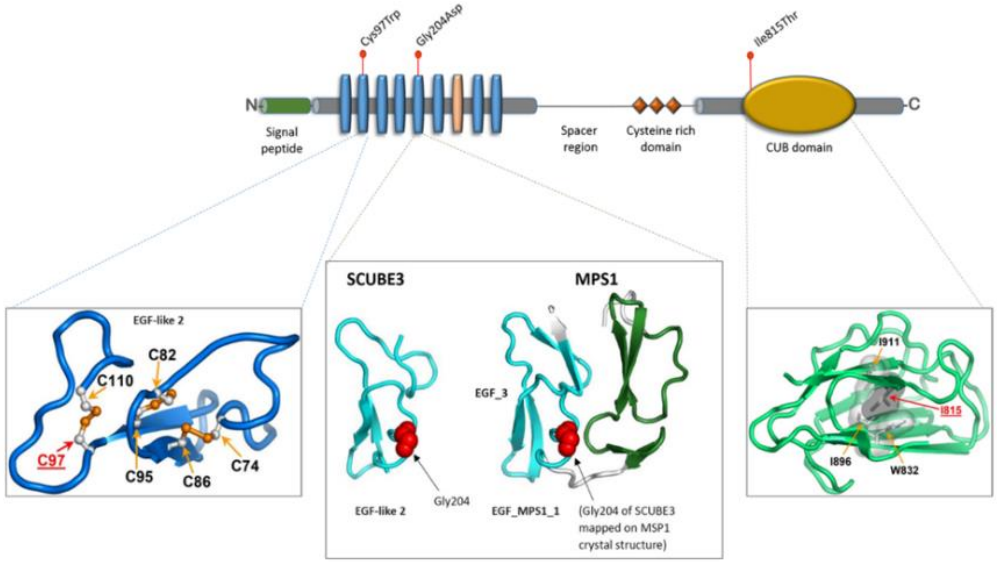

EGF-like2

SCUBE3	*H.sapiens*	DVDECERE-DNAGCVHDCVNIPGNYRCTCYDGFHLAHDGHNCL
Scube3	*P.troglodytes*	DVDECERE-DNAGCVHDCVNIPGNYRCTCYDGFHLAHDGHNCL
Scube3	*C.lupus*	DVDECERE-DNAGCVHDCVNIPGNYRCTCYDGFHLAHDGHNCL
Scube3	*B.taurus*	DVDECERE-DNAGCVHDCVNIPGNYRCTCYDGFHLAHDGHNCL
Scube3	*M.musculus*	DVDECERE-DNAGCVHDCVNIPGNYRCTCYDGFHLAHDGHNCL
Scube3	*R.norvegicus*	DVDECERE-DNAGCVHDCVNIPGNYRCTCYDGFHLAHDGHNCL
Scube3	*G.gallus*	DVDECERE-DNAGCVHECVNIPGNYRCTCYDGFRLAHDGHNCL
Scube3	*D.rerio*	DIDECASE-YNGGCVHECINIPGNYRCTCYDGFHLAHDGHNCL
SCUBE1	*H.sapiens*	DIDECENDYYNGGCVHECINIPGNYRCTCFDGFMLAHDGHNCL
SCUBE2	*H.sapiens*	DIDECGNE-LNGGCVHDCLNIPGNYRCTCFDGFMLAHDGHNCL
LTBP3	*H.sapiens*	DVDECEAG-DVCD-NGICSNTPGSFQCQCLSGYHLSRDRSHCE
FBN2	*H.sapiens*	DVDECEIGAHNCDMHASCLNIPGSFKCSCREGW--IGNGIKCI
FBN1	*H.sapiens*	DINECEIGAHNCGKHAVCTNTAGSFKCSCSPGW--IGDGIKCT

EGF-like5

SCUBE3	*H.sapiens*	--LTCNYGNGGCQHTCDDTEQGPRCGCHIKFVLHTDGKTCI
Scube3	*P.troglodytes*	----------CL
Scube3	*C.lupus*	--LTCNYGNGGCQHTCDDTEQGPRCGCHVKFVLHTDGKTCI
Scube3	*B.taurus*	--LTCNYGNGGCQHTCDDTEQGPRCGCHVKFVLHTDGKTCI
Scube3	*M.musculus*	--LTCNYGNGGCQHTCDDTEQGPRCGCHVKFVLHTDGKTCI
Scube3	*R.norvegicus*	--LTCNYGNGGCQHTCDDTEQGPRCGCHVKFVLHTDGKTCI
Scube3	*G.gallus*	--LTCNYGNGGCQHTCDDTDQGPKCGCHVKFLLHSDGVTCI
Scube3	*D.rerio*	--LTCNYGNGGCQHICEETDHGPKCSCHMKFALHSDGKTCV
SCUBE1	*H.sapiens*	----CNYGNGGCQHSCEDTDTGPTCGCHQKYALHSDGRTC-
SCUBE2	*H.sapiens*	----CNHGNGGCQHSCDDTADGPECSCHPQYKMHTDGRSC-
LTBP3	*H.sapiens*	DVDECEIGAHNCDMHASCLNIPGSFKCSCREGWIGNGIKCI
FBN2	*H.sapiens*	DVDECEIGAHNCDMHASCLNIPGSFKCSCREGWIGNGIKCI
FBN1	*H.sapiens*	DINECEIGAHNCGKHAVCTNTAGSFKCSCSPGWIGDGIKCT

CUB

SCUBE3	*H.sapiens*	CGGELGEFTGYIESPNYPGNYPAGVECIWNIN
Scube3	*P.troglodytes*	CGGELGEFTGYIESPNYPGNYPAGVECIWNIN
Scube3	*C.lupus*	CGGELGEFTGYIESPNYPGNYPAGVECVWNIN
Scube3	*B.taurus*	CGGELGEFTGYIESPNYPGNYPAGVECVWNIN
Scube3	*M.musculus*	CGGELGEFTGYIESPNYPGNYPAGVECVWNIN
Scube3	*R.norvegicus*	CGGELGEFTGYIESPNYPGNYPAGVECIWNIN
Scube3	*G.gallus*	CGGELGEYTGYIESPNYPGNYPANVECTWNIN
Scube3	*D.rerio*	CGGEIGEFIGYIESPNYPGNYPANVECVWTIN
SCUBE1	*H.sapiens*	CGGELGDYTGYIESPNYPGDYPANAECVWHIA
SCUBE2	*H.sapiens*	CGGELGDFTGYIESPNYPGNYPANTECTWTIN
KREMEN1	*H.sapiens*	CGGELGEFTGYIESPNYPGNYPAGVECIWNIN
BMP1	*H.sapiens*	CGGDVKKDYGHIQSPNYPDDYRPSKVCIWRIQ

Figure S4. Structural analyses.

The homology model shows the 2nd EGF-like domain with the invariant Cys^{97} and the other disulfide-forming cysteines. Substitution of Cys^{97} implies loss of one of the three conserved disulfide bridges of the motif (left). Homology model of the 5th EGF-like domain with the conserved Gly^{204}. The nonconservative substitution is predicted to impair proper module folding, and impact the interaction with the adjacent EGF-like module (middle). Homology model of the CUB domain is shown with location of Ile^{815} and surrounding residues (Trp^{832}, Ile^{896}, and Ile^{911}) forming a cluster of buried hydrophobic amino acids in the core of the domain. The introduction of a polar residue is predicted to considerably destabilize the structure of the entire domain (right). Conservation of affected residues in orthologs, paralogs and structurally related proteins is also shown.

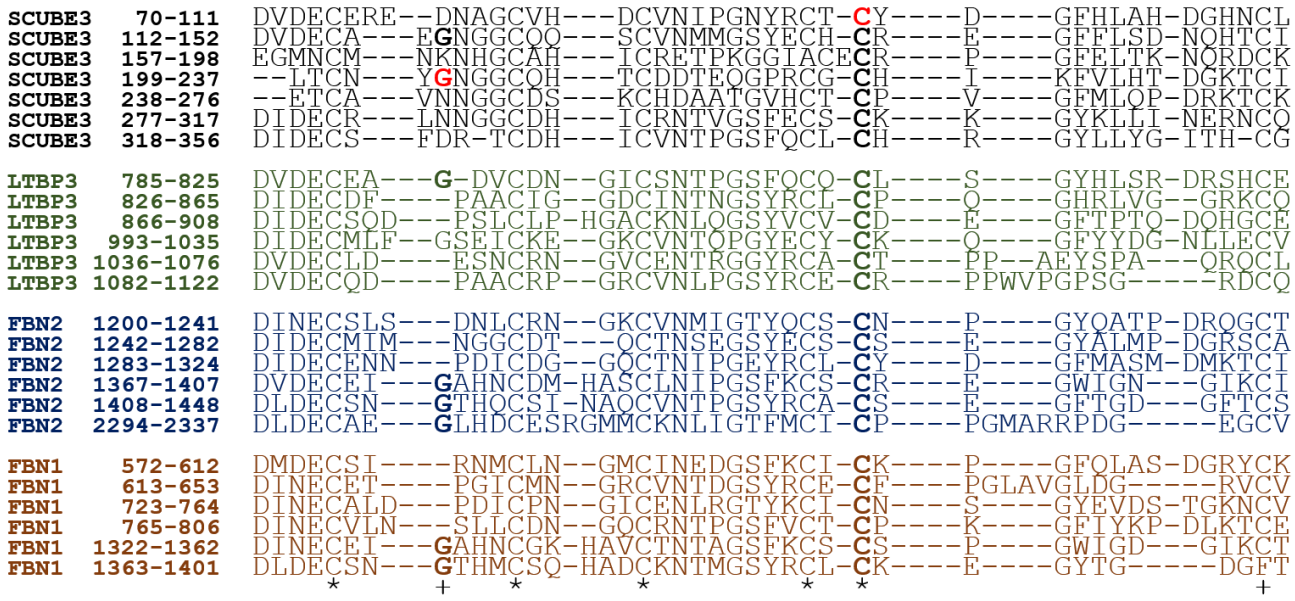

Figure S5. Alignments of the SCUBE3 EGF-like modules with equivalent modules of the LTBP3, FBN2 and FBN1 proteins.

Multiple sequence alignment of EGF-like meta-domains around the sites of the Cys^{97} and Gly^{204} (2^{nd} and 5^{th} EGF-like module of SCUBE3, respectively). (*) identical residues; (+) conserved residues.

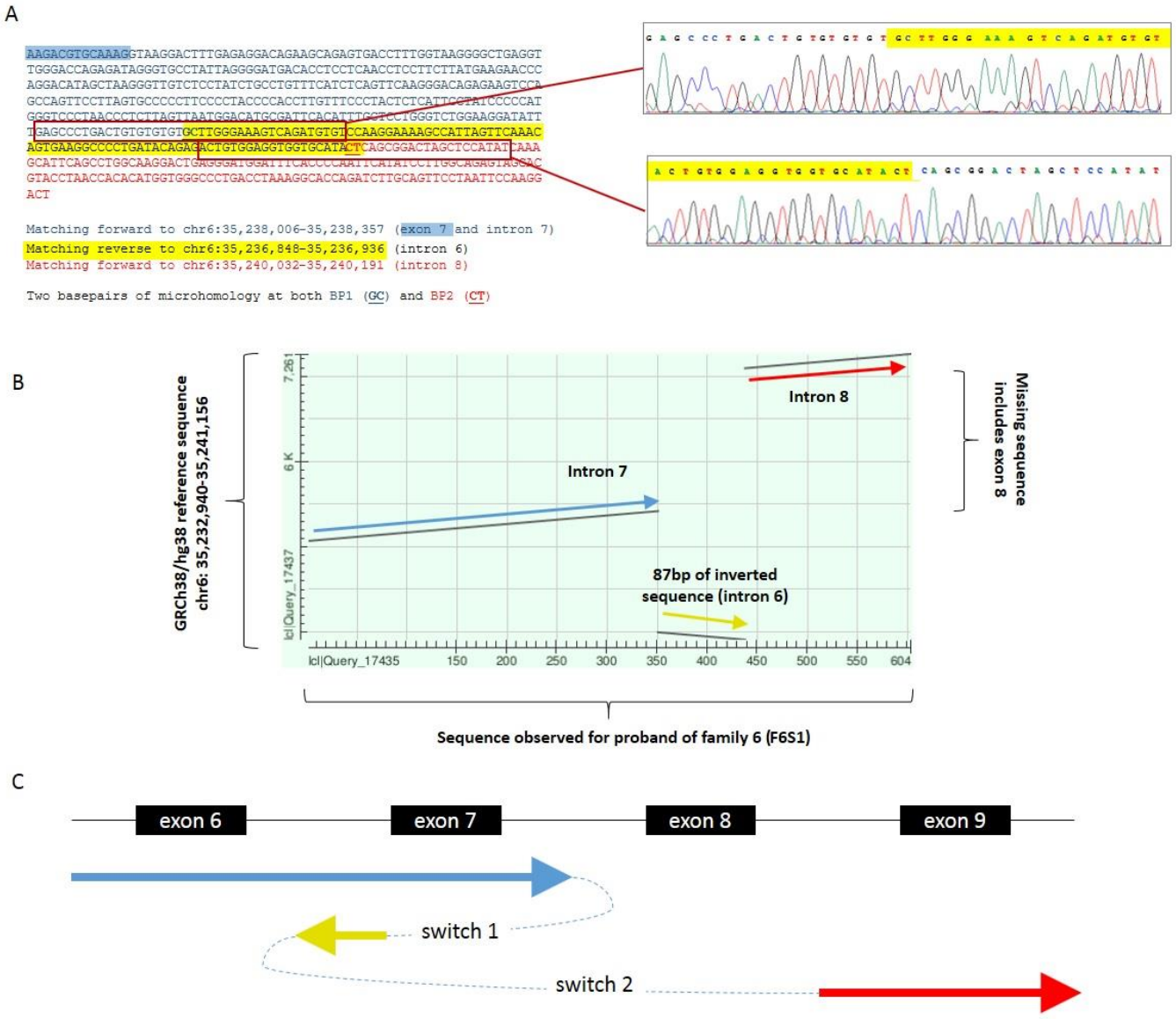

Figure S6. Breakpoints and characterization of the intragenic *SCUBE3* rearrangement involving exon 8 (family 6).

(A) Breakpoints of the rearrangement were confirmed by Sanger sequencing.

(B) Dotplot comparing rearrangement to reference sequence, generated using BLASTN tool (https://blast.ncbi.nlm.nih.gov/).

(C) Schematic diagram of the *SCUBE3* rearrangement. This complex rearrangement (deletion plus inverted duplication) likely originated from a two-step fork-switching and template-stalling (FoSTeS) process (also designated microhomology-mediated break-induced repair, MMBIR).

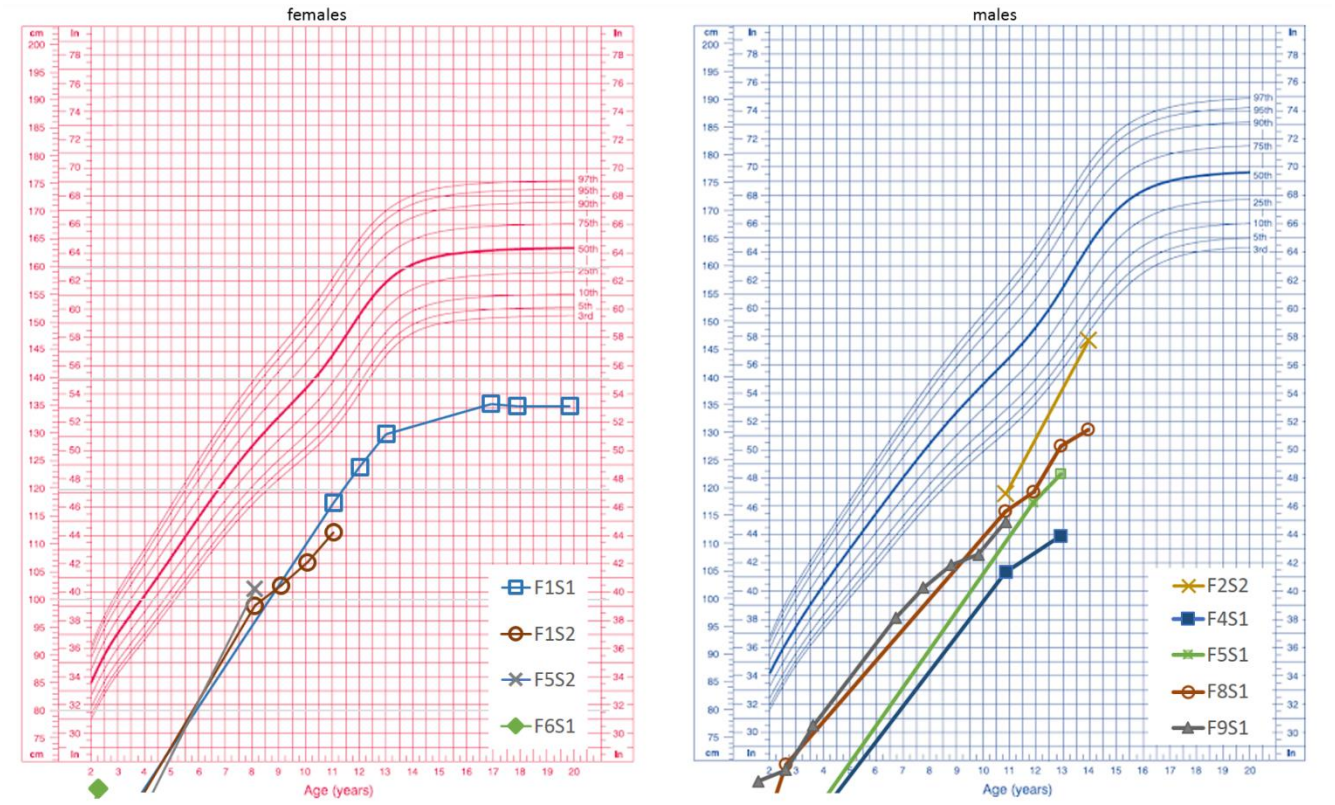

Figure S7. Growth pattern in subjects with biallelic inactivating *SCUBE3* variants. Height data are plotted on the 2000 CDC growth charts (Kuczmarski et al. 2002).

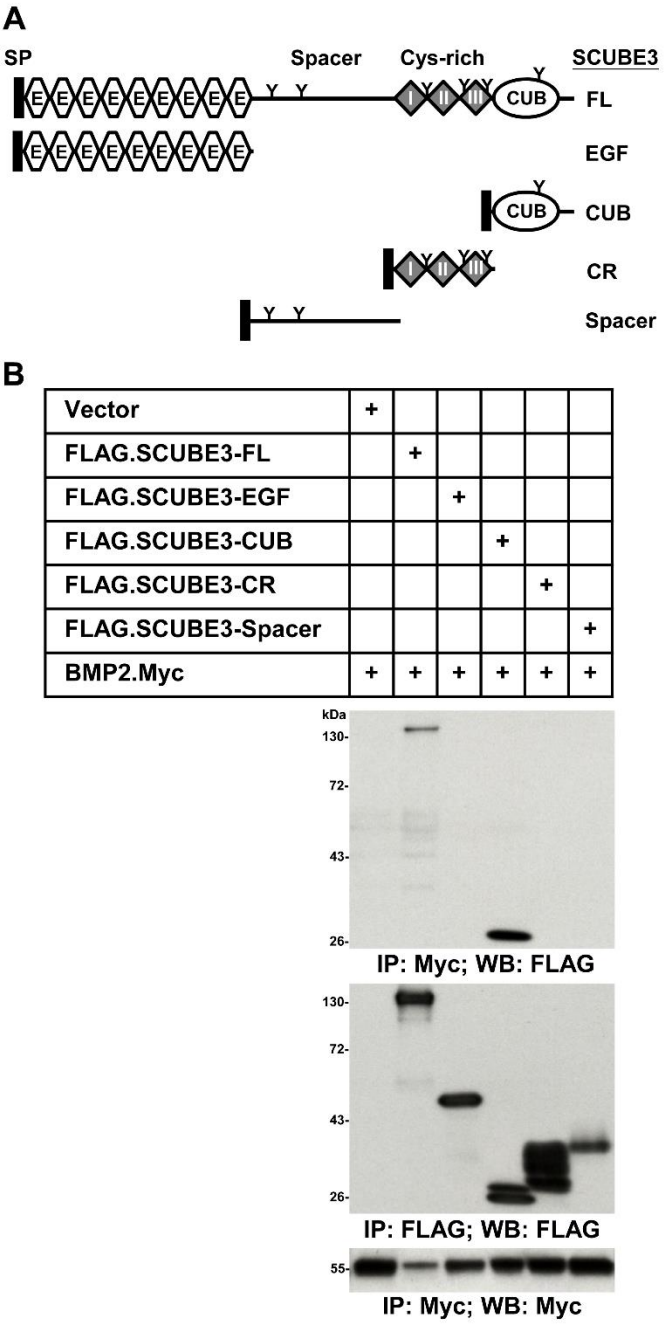

Figure S8. Molecular mapping of the interacting domains between SCUBE3 and BMP2.

(A) Domain organization of the SCUBE3 expression constructs used to map the interacting domains. A FLAG epitope was added immediately after the signal peptide sequence at the NH_2 terminus of each construct. SP, signal peptide; CR, cysteine-rich.

(B) The CUB domain of SCUBE3 interacts with BMP2. The expression plasmids encoding Myc-tagged BMP2 were transfected alone or with a series of FLAG-tagged SCUBE3 constructs in HEK-293T cells. After 48 h, cell lysates underwent immunoprecipitation, followed by western blot analysis with indicated antibodies to determine protein–protein interactions. IP, immunoprecipitation; WB, western blotting. Representative blots from one experiment of three performed are shown.

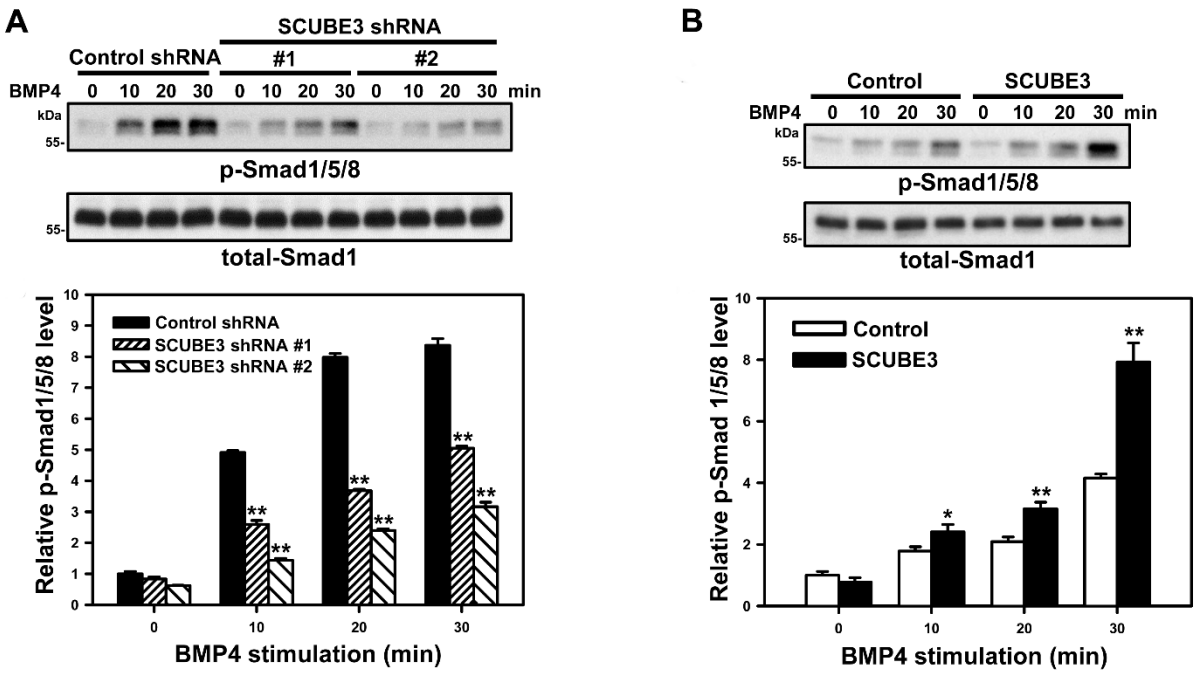

Figure S9. SCUBE3 enhances BMP4-stimulated osteoblast differentiation in C3H10T1/2 cells.
(A) *SCUBE3* knockdown impairs BMP4 signaling in C3H10T1/2 cells. Endogenous *SCUBE3* expression was inhibited by two different *SCUBE3*-targeting short hairpin RNA (shRNA) lentiviruses (SCUBE3-shRNA #1 or #2) in C3H10T1/2 cells. A luciferase shRNA lentivirus was used as a negative control (control-shRNA). Efficiency of *SCUBE3* knockdown and its effect on the phosphorylation of Smad1/5/8 were assessed by western blot analysis with total-Smad1 expression used as an internal control (above). Quantification of BMP4-induced phosphorylation of Smad1/5/8 in control or *SCUBE3* knockdown C3H10T1/2 cells. Data are mean ± SD from three independent experiments. **, P <0.01 compared to control (below).
(B) *SCUBE3* overexpression enhances BMP4 downstream signaling in C3H10T1/2 cells. Exogenous *SCUBE3* expressed in C3H10T1/2 cells transduced with an empty lentivirus or recombinant lentivirus encoding an FLAG-tagged SCUBE3. Western blot analysis (above) and quantification (below) of BMP4-induced phosphorylation of Smad1/5/8 with control and SCUBE3 overexpression in C3H10T1/2 cells. Data are mean ± SD from three independent experiments. *P <0.05; **, P < 0.01 compared with control.

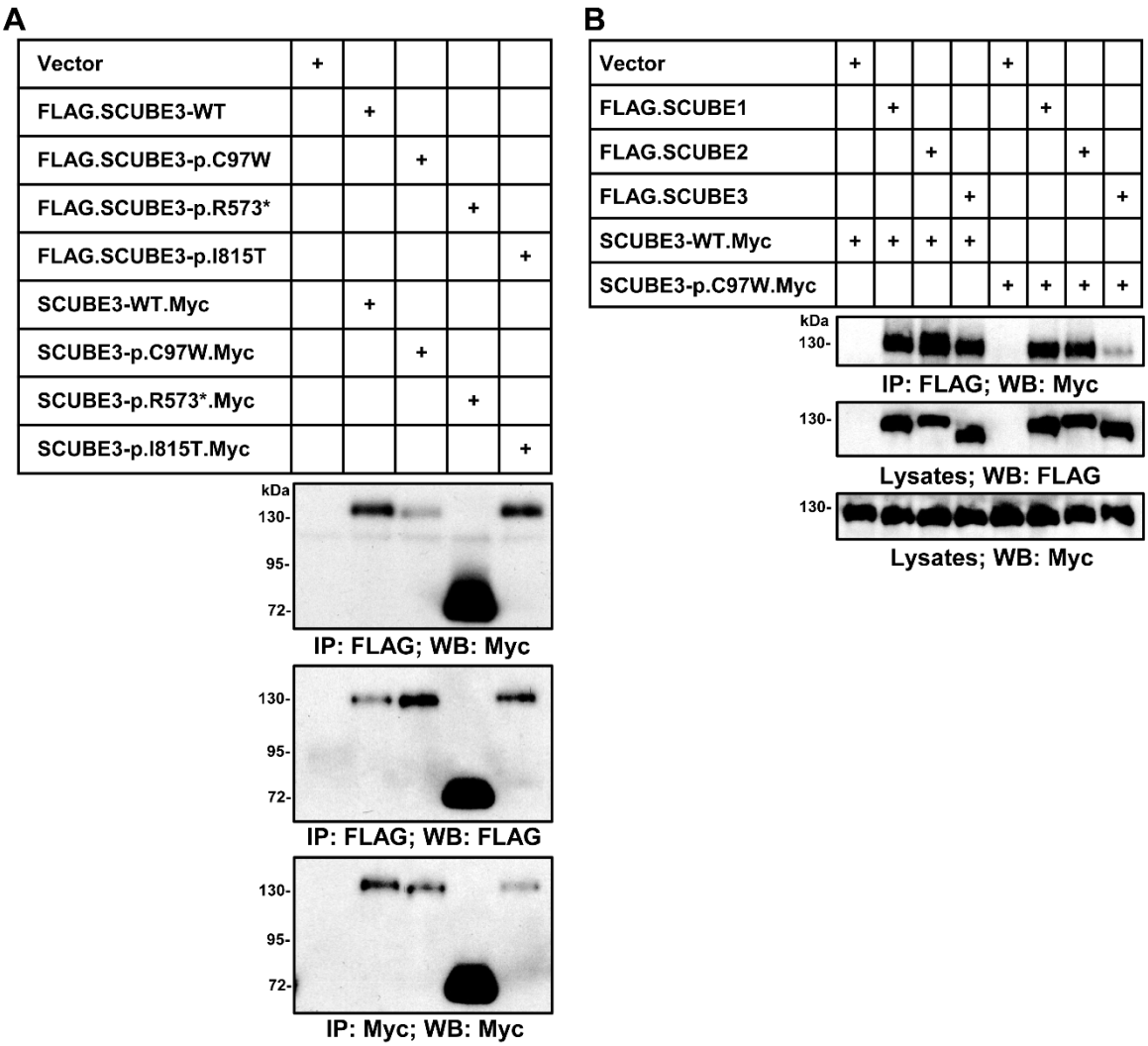

Figure S10. Effect of *SCUBE3* mutations on WT-mutant or mutant-mutant oligomerizations.

(A) Homodimerization assays. HEK-293T cells were transfected with expression plasmids encoding FLAG-tagged wild-type *SCUBE3* or individual mutants pCys97Trp (p.C97W), p.Arg573* (p.R573*) or p.Ile815Thr (p.I815T) together with their corresponding Myc-tagged constructs. Representative blots from one experiment of three performed are shown.

(B) Heterodimerization assays. HEK-293T cells were transfected with the expression plasmids encoding FLAG-tagged SCUBE1, SCUBE2 or SCUBE3 together with Myc-tagged wild-type SCUBE3 or the p.Cys97Trp (p.C97W) SCUBE3 mutants.

Lysates of transfected cells were immunoprecipitated (IP) with an anti-FLAG antibody, and associated protein levels were determined by western blot (WB) analysis with an anti-Myc antibody (top panels). The expression of FLAG or Myc-SCUBE3-WT, C97W, R573* or I815T proteins was verified by anti-FLAG or anti-Myc western blot analysis, respectively (second and third panels). Representative blots from one experiment of three performed are shown.

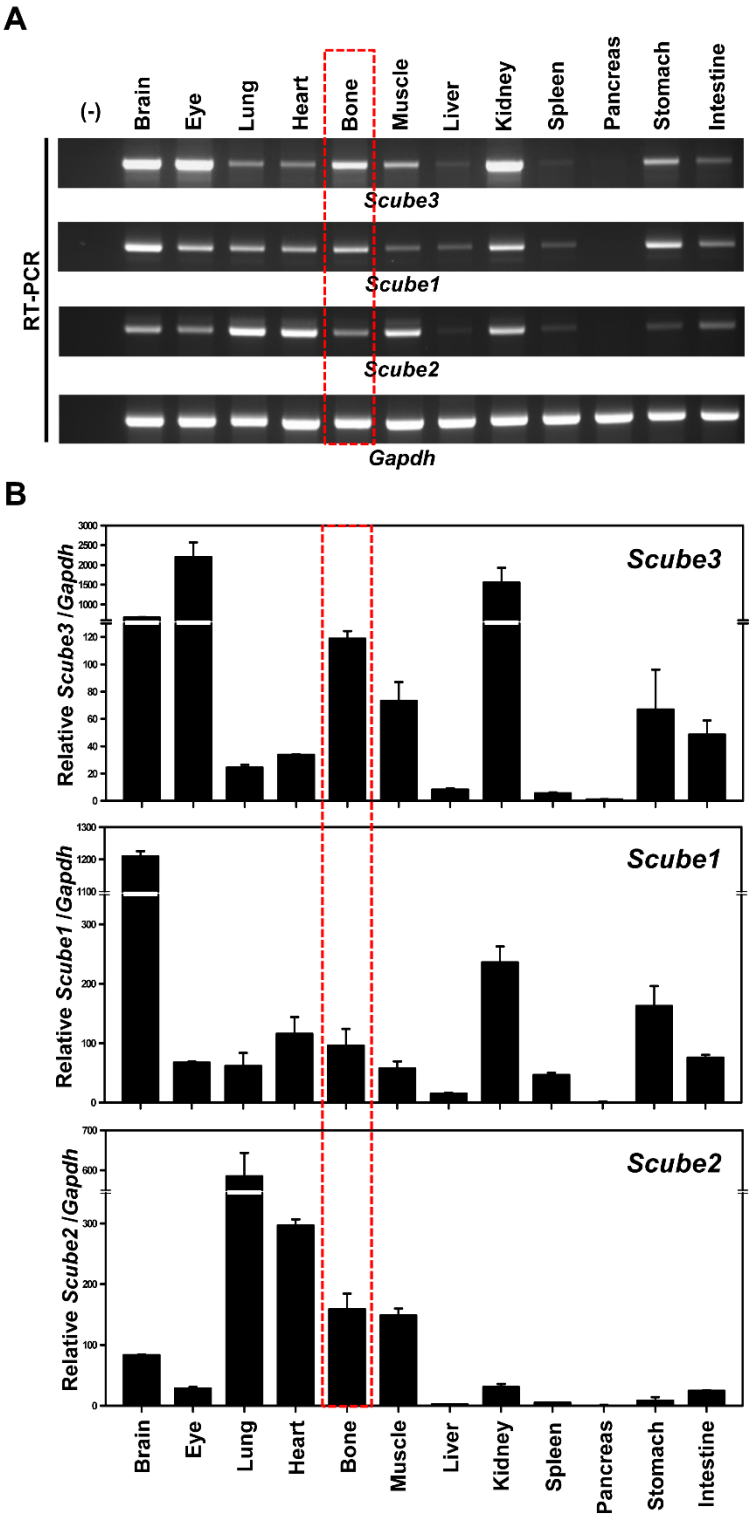

Figure S11. Expression of *Scube* genes in major organs in wild-type newborn mice.
RT-PCR **(A)** and quantitative RT-PCR **(B)** analyses of the expression of *Scube* genes in P1 newborn mice. First-strand cDNAs from brain, eye, lung, heart, bone, muscles, liver, kidney, spleen, pancreas, stomach, and intestine were used for RT-PCR and quantitative RT-PCR with primers specific for each *Scube* gene. Expression of *Gapdh* was used an internal control. Data are mean ± SD from three independent experiments.

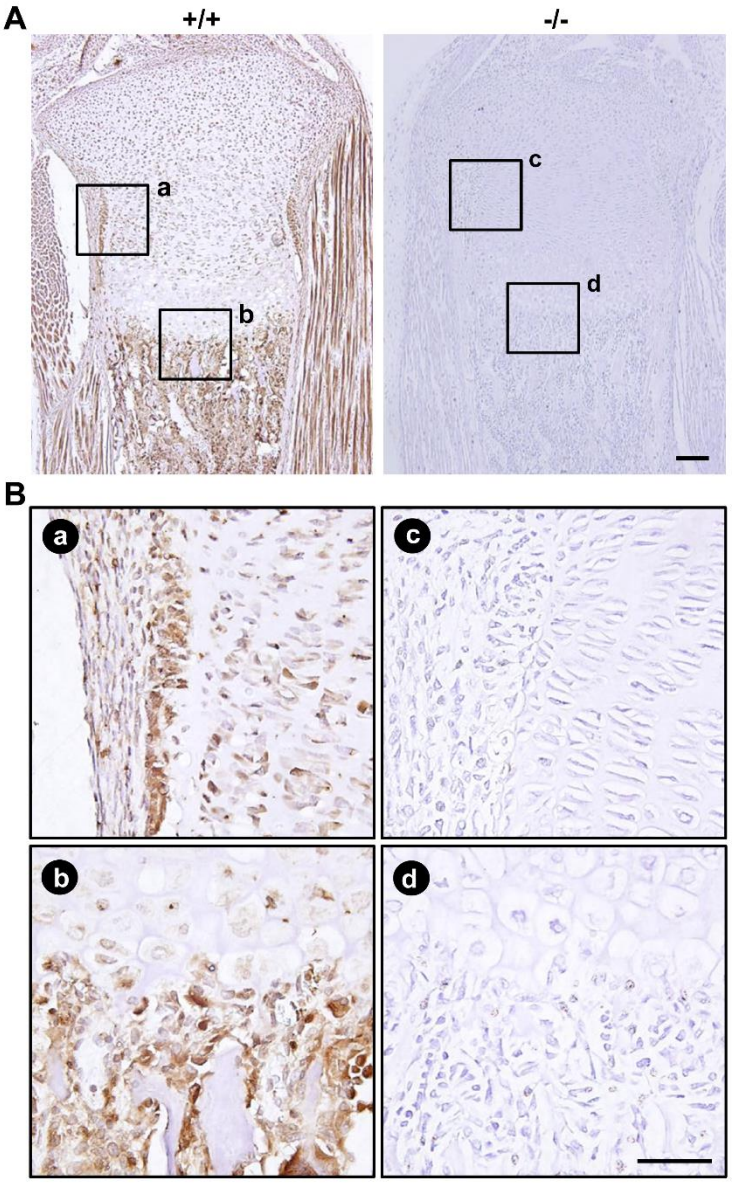

Figure S12. Immunohistochemical localization of SCUBE3 in neonatal mouse bone tissues.
(A) Sections of neonatal (P1) wild-type (+/+) or mutant (-/-) mouse tibiae were stained with a rabbit polyclonal antibody for SCUBE3.
(B) High-power images showing anti-SCUBE3 immunostaining localized in the periosteum (panel a), proliferative/prehypertrophic chondrocytes, and trabecular region (panel b) of +/+ mice, with immunoreactivity completely absent in -/- bones (panels c and d). Scale bars = 100 µm.

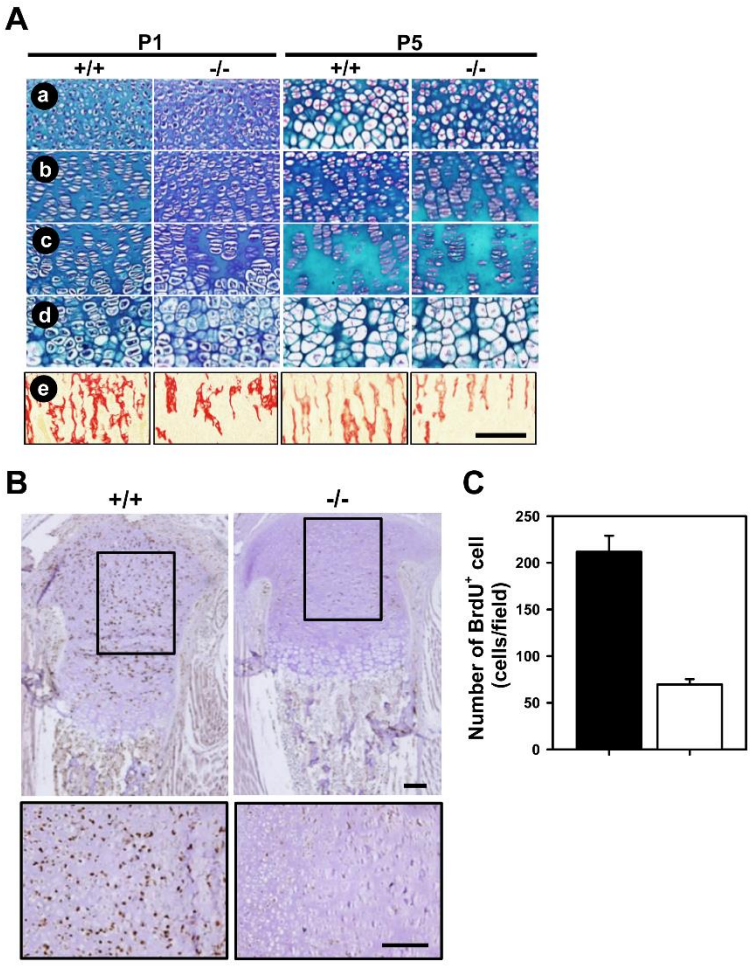

Figure S13. Effect of Scube3 knockout on the structure of growth plates and chondrocyte proliferation.

(A) Alcian blue hematoxylin/orange G of proximal tibia with resting chondrocytes (a), proliferative chondrocytes (b), prehypertrophic chondrocytes (c), and hypertrophic chondrocytes (d) of growth-plate chondrocytes. Cartilage: blue/purple (glycosaminoglycan /proteoglycan); bone: orange; erythrocytes or soft tissues: pink to red (a-d). Total collagen staining of proximal tibia with osteoblast/blood vessels of growth-plate chondrocytes (e). Scale bar =100 μm.

(B and C) Immunohistochemistry of tibiae from BrdU-labeled +/+ and -/- neonatal pups (P1) by using anti-BrdU antibody. Magnified views of the boxed periarticular regions are shown in the same columns (B). BrdU-positive cell number was counted and expressed as BrdU-positive cells/field in the periarticular regions of each section (C). **, $P < 0.01$ (n=5 animals in each genotype group). Scale bar = 100 μm.

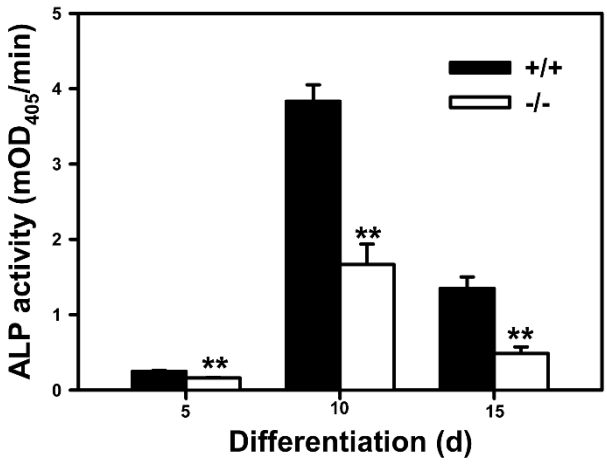

Figure S14. *Ex vivo* osteogenic differentiation of +/+ or -/- embryonic (E18.5) osteoblastic cells assessed by ALP activity.

ALP activity of +/+ and -/- embryonic osteoblastic cells under osteoblast differentiation conditions at days 5, 10, and 15. The experiments were performed 3 times in triplicate with similar results. Data are mean ± SD. mOD_{405}, milli-absorbance units at 405 nm. **, $P < 0.01$.

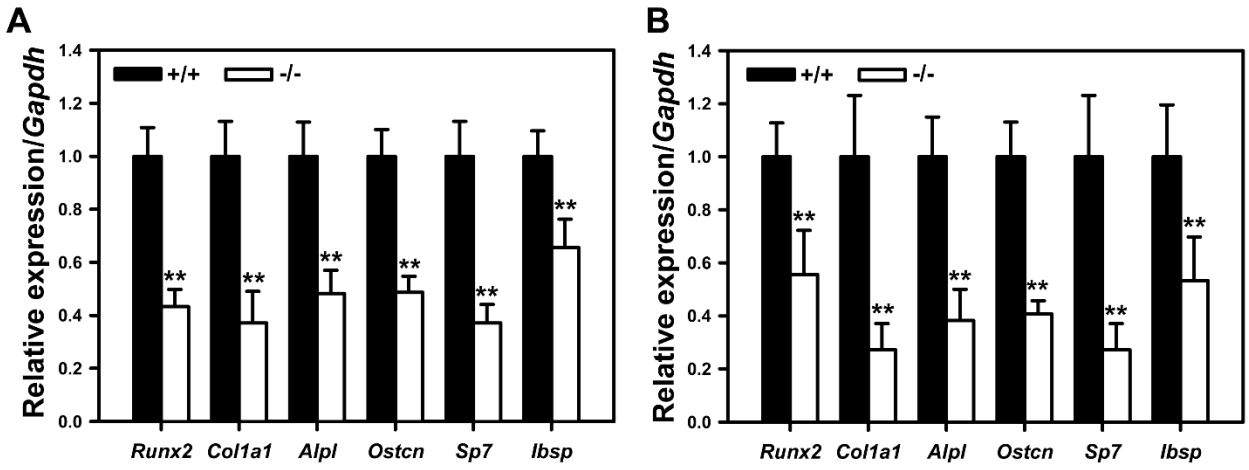

Figure S15. *SCUBE3* knockout reduces the expression of osteogenic marker genes in primary cultured chondrocytes and isolated long bones from +/+ or -/- animals.

Quantitative real-time RT-PCR of osteogenic phenotype markers in primary cultured chondrocytes **(A)** and long bones of hindlimbs **(B)** from +/+ or -/- animals (P2). Expression of osteoblast marker genes, Runt-related transcription factor 2 (*Runx2*, a transcriptional activator of osteoblast differentiation), type I collagen α1 chain (*Col1a1*), alkaline phosphatase (*Alpl*), osteocalcin (*Ostcn*), osterix (also named *Sp7*, a bone specific transcription factor essential for osteoblast differentiation and bone formation), and bone sialoprotein (*Bsp*, also known as integrin-binding sialoprotein *Ibsp*; a major structural protein of the bone matrix), are normalized to *Gapdh* mRNA level. Data are mean ± SD (n=5 in each group). **, $P < 0.01$.

Supplemental Figure 15

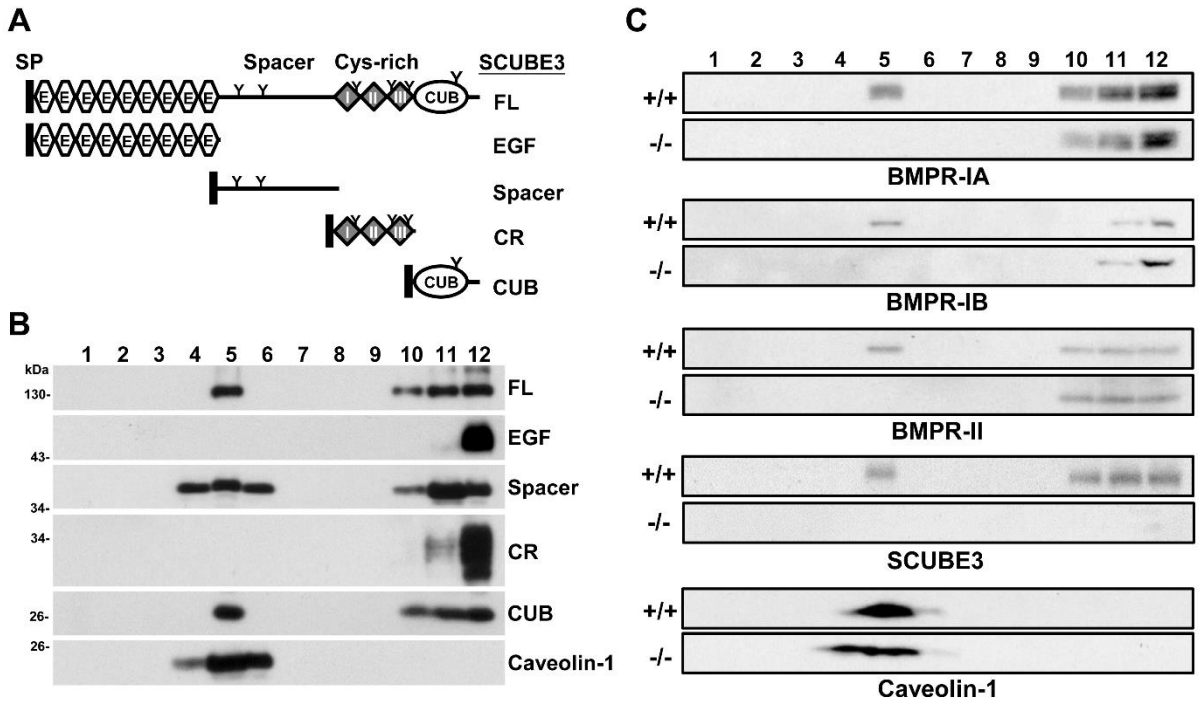

Figure S16. Requirement of SCUBE3 for stimulus-dependent BMP receptor association with lipid rafts.

(A and **B)** The spacer and CUB domain of SCUBE3 is crucial for lipid raft association. Domain organization of the SCUBE3 expression constructs used to map lipid raft-associated domains. The FLAG epitope was added immediately after the signal peptide sequence at the NH2-terminus of SCUBE3 constructs. SP, signal peptide; CR, cysteine-rich (a). SCUBE3-FL, Spacer, and CUB domain detected in lipid raft fraction. The expression plasmids encoding a series of FLAG-tagged SCUBE3 constructs were transfected in HEK-293T cells for 2 days; cell lysates underwent ultracentrifugation analysis and were collected as 12 fractions. Each fraction was examined by western blot analysis with anti-FLAG antibody. Fraction 5, which is enriched in caveolin-1, a marker of lipid raft, represents the lipid raft fraction (b). Representative blots from one experiment of three performed are shown.

(C) Abolished lipid raft association of BMP receptors (IA, IB, and II) in -/- chondrocytes in response to BMP2. Primary cultured chondrocytes were treated with 100 ng/ml BMP2 for 60 min. Cell lysates underwent ultracentrifuge analysis and were collected as 12 fractions. Each fraction was examined by western blot analysis with the indicated antibodies. Representative blots from one experiment of three performed are shown.

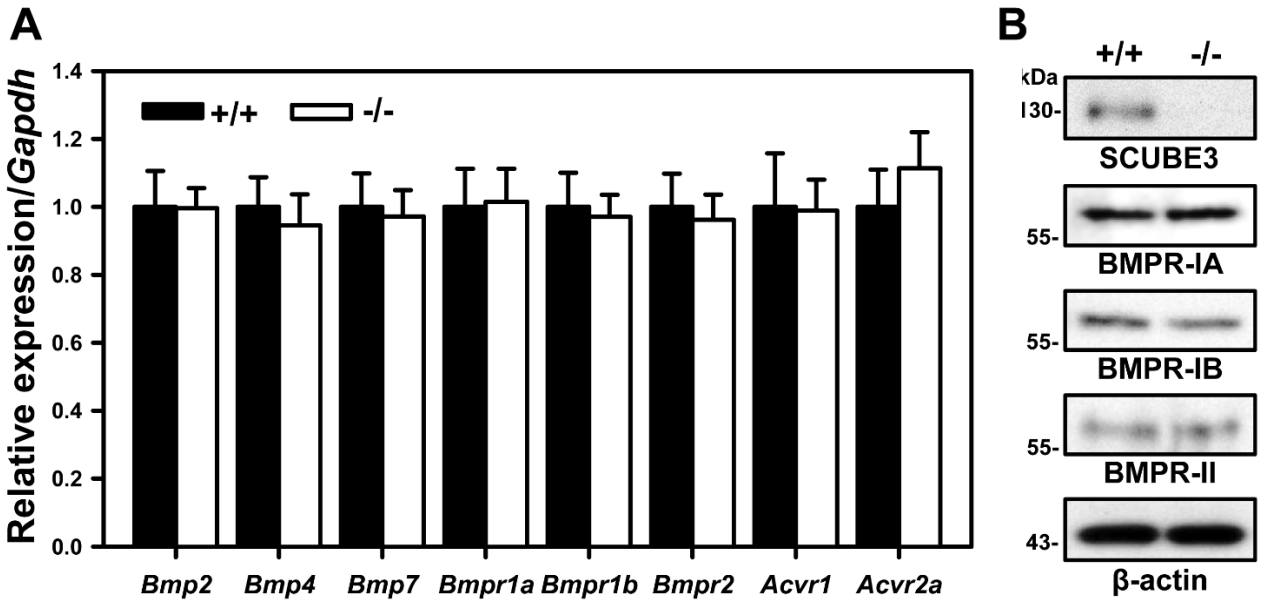

Figure S17. Expression of BMP signaling components and BMP receptor protein in primary cultured chondrocytes.

(A) Quantitative real-time RT-PCR of BMP signaling components in primary cultured chondrocytes from *Scube3*$^{+/+}$ or *Scube3*$^{-/-}$ animals (P2). Expression of BMP pathway genes, including bone morphogenetic protein 2 (*Bmp2*), bone morphogenetic protein 4 (*Bmp4*), bone morphogenetic protein 7 (*Bmp7*), bone morphogenetic protein receptor type 1a (*Bmpr1a*), bone morphogenetic protein receptor type 1b (*Bmpr1b*), bone morphogenetic protein receptor type 2 (*Bmpr2*), activin A receptor type 1 (*Acvr1*), and activin A receptor type 2a (*Acvr2a*), was normalized to *Gapdh* mRNA level. Data are mean ± SD (n=5 in each group). **, $P < 0.01$.

(B) *Scube3* knockout did not alter BMP receptor protein levels in primary cultured chondrocytes. Western blot analysis of the protein expression of BMP receptors in primary cultured chondrocytes. β-actin level was used as loading control. Representative blots from one experiment of three performed are shown.

Table S1. WES statistics and data output.

Subject F1S1 (Italy) (singleton)	
WES Enrichment Kit	Nextera Rapid Capture Kit
Sequencing Platform	NextSeq 550
Target regions coverage, 10x	94.9%
Target regions coverage, 20x	91.1%
Average sequencing depth on target	76x
Candidate disease genes (autosomal recessive inheritance)[1]	4[2]
Putative disease gene	1, *SCUBE3*
Subject F2S1 (India) (singleton)	
WES Enrichment Kit	Ion AmpliSeq Exome RDY Kit
Sequencing Platform	Ion Proton
Target regions coverage, 10x	98.5%
Target regions coverage, 20x	97.5%
Average sequencing depth on target	208x
Candidate disease genes (recessive inheritance)[1]	1[3]
Putative disease gene	1, *SCUBE3*
Subject F3S1 (Iran) (singleton)	
WES Enrichment Kit	Nextera Rapid Capture Kit
Sequencing Platform	NextSeq 500
Target regions coverage, 10x	94.4%
Target regions coverage, 20x	86.5%
Average sequencing depth on target	63x
Candidate disease genes (autosomal recessive inheritance)[1]	4[4]
Putative disease gene	1, *SCUBE3*
Subject F4S1 (UK) (trio)	
WGS library preparation	Illumina TruSeq DNA PCR-Free
Sequencing Platform	HiSeq X
Target regions coverage, 10x	99.7%
Target regions coverage, 20x	99.2%
Average sequencing depth on target	43x
Candidate disease genes (recessive inheritance)[5]	28
Candidate disease genes (autosomal dominant inheritance)	0
Putative disease gene	1[6], *SCUBE3*
Subject F5S1 (Turkey) (duo, affected sibs)	
WES Enrichment Kit	Agilent Sure Select XT V5
Sequencing Platform	HiSeq 4000
Target regions coverage, 10x	98.20%
Target regions coverage, 20x	93.59%
Average sequencing depth on target	79.0x
Candidate disease genes (autosomal recessive inheritance)[1]	1[7]
Putative disease gene	1, *SCUBE3*

Subject F6S1 (Saudi Arabia) (trio)	
WGS library preparation	Illumina TruSeq DNA PCR-Free
Sequencing Platform	HiSeq X
Target regions coverage, 10x	98.6
Target regions coverage, 20x	97.7
Average sequencing depth on target	38x
Candidate disease genes (autosomal recessive inheritance)[1]	1[8]
Putative disease genes	1, *SCUBE3*
Subject F7S1 (United Arab Emirates) (trio)	
WES Enrichment Kit	Agilent SureSelect Human All Exon V6
Sequencing Platform	HiSeq 4000
Target regions coverage, 10x	99.2
Target regions coverage, 20x	97.7
Average sequencing depth on target	153x
Candidate disease genes (recessive inheritance)[1]	NA[9]
Candidate disease genes (dominant inheritance)	0
Putative disease gene	1, *SCUBE3*
Subject F8S1 (Brazil) (singleton)	
WES Enrichment Kit	Agilent Sure Select All Exon V6
Sequencing Platform	HiSeq 2500
Target regions coverage, 10x	99.2%
Target regions coverage, 20x	97.5%
Average sequencing depth on target	132.9x
Candidate disease genes (recessive inheritance)[1]	3[10]
Putative genes (autosomal recessive inheritance)	1, *SCUBE3*
Subject F9S1 (Israel) (singleton)	
WES Enrichment Kit	Twist plus
Sequencing Platform	Illumina HiSeq 2500
Target regions coverage, 10x	96%
Target regions coverage, 20x	95%
Average sequencing depth on target	250
Novel/low frequency variants with predicted functional effect[1]	152
Putative disease genes (autosomal recessive inheritance)	4 (*SCUBE3, BTN2A2,ZNRD1,PPP1R10*)[11]

[1]Filtering retained genes with rare (MAF<0.1% gnomAD v.2.0, and <2% in house database [1,600 population-matched exomes]) variants, excluding those predicted as benign by CADD (scaled score <15) and M-CAP (score < 0.025) algorithms or considered as benign/likely benign by interVar (F1S1); filtering retained high-quality rare and clinically associated variants affecting coding exons and splice sites with MAF<0.1% in local and public databases and CADD score > 20 (F2S1); filtering retained genes with rare (MAF<0.1% each used for gnomAD v.2.0 and GME, and <2% in house database [130 exomes]) variants, excluding those predicted as benign by CADD (scaled score <15) and M-CAP (score < 0.025) algorithms or considered as benign/likely benign by interVar (F3S1); filtering retained high-quality rare and clinically associated variants affecting coding exons and splice sites with MAF<0.1% (or 2% for compound-heterozygotes) in all of the following reference databases: 100,000 Genomes Project reference samples, 1000 Genomes, ESP, TOPMed, UK10K, ExAC and gnomAD (excluding the Ashkenazi Jewish population), and prioritizing by a logistic regression model by using Exomiser tool (F4S1); high-quality nonsynonymous variants (excluding missense variants with a low PhyloP score) and variants within splice sites (+/-2) with frequency of <3% in gnomAD and GoNL databases and <2% in in-house database (F5S1); filtering retained genes with rare (MAF<0.1% in gnomAD v.2.0, and in house [approx. 70,000 exomes and genomes] databases) variants, excluding those predicted as benign by CADD (scaled score <15); filtering was not performed because of direct matching after considering *SCUBE3* as a novel clinically associated gene implicated in syndromic skeletal disorder (F7S1); filtering retained genes with rare

(MAF<0.1% in gnomAD v.2.0, ABraOM [approx. 600 exomes] and in house [approx. 750 population-matched exomes] databases) variants, excluding those predicted as benign by CADD (scaled score <15) and M-CAP (score < 0.025) algorithms or considered as benign/likely benign by interVar (F8S1); filtering retained genes with rare (MAF <0.1% in gnomAD V. 2.0 database and <2% in in-house database (population-matched 3500 exomes), and functionally relevant variants by excluding variants predicted as benign by CADD (scaled score <15) or benign/likely benign by Varsome (F9S1).

[2]*SCUBE3* (c.291C>G, p.Cys97Trp; CADD = 26.1), *TSC2* (c.649-7C>T; CADD = 4.5), *BFAR* (c.77A>G, p.Gln26Arg; CADD = 19.6), *CHRDL2* (c.432+8C>A, CADD = 8.8; c.195+3_195+10delAGGTTCCT; CADD = 14.9).

[3]*SCUBE3* (c.2444T>C, p.Ile815Thr; CADD=27.9).

[4]*SCUBE3* (c.1717C>T, p.Arg573*; CADD = 39), *ITPR1* (c.2183G>A, p.Arg728Gln; CADD 22.3), *HMCN2* (c.686C>A, p.Asp228Glu; CADD 24.9), *PCIF1* (c.1292G>A, p.Arg431Gln; CADD 24).

[5]According to TIERING table performed as described previously, see PMID: 29691228 and https://doi.org/10.6084/m9.figshare.4530893.v4.

[6]*SCUBE3* (c.2239+1G>A, p.Val747Aspfs*46; CADD = 34).

[7]*SCUBE3* (c.2599+2T>C; CADD = 27.2).

[8]*SCUBE3* (c.829+1_952del, p.Arg282_Cys322del; CADD, NA).

[9]*SCUBE3* (c.2444T>C, p.Ile815Thr; CADD = 27.9).

[10]*SCUBE3* (c.611G>A, p.Gly204Asp; CADD = 26.2); *TRAF3IP2* (c.440c>T, p.Ala147Val; CADD = 32); *SNTA1* (c.160G>C, p.Gly54Arg; CADD = 22.9)

[11]*SCUBE3* (c.2782C>T, p.R928*; CADD = 45); *BTN2A2* (c.583C>T, p.Q195*; CADD = 27.9); *ZNRD1 (*c.356+3G>A; near to splice site); *PPP1R10* (c.194+8G>C; near to splice site).

Table S2. Key resources

REAGENT or RESOURCE	SOURCE	IDENTIFIER
Antibodies		
Anti-ALP	GeneTex	GTX62596
Anti-BMPR-IA	abcam	ab59947
Anti-BMPR-IB	abcam	ab175385
Anti-BMPR-II	Santa Cruz Biotechnology	sc-20737
Anti-BrdU	GeneTex	GTX26326
Anti-Caveolin-1	Santa Cruz Biotechnology	sc-894
Anti-FLAG	Cell Signaling Technology	CST #14793
Anti-FLAG M2	SIGMA	F1804
Anti-HA	Cell Signaling Technology	CST #3724
Anti-Myc	Cell Signaling Technology	CST #2276
Anti-Osteocalcin	Santa Cruz Biotechnology	sc-30045
Anti-phospho-Smad1/5/8	Cell Signaling Technology	CST #9511
Anti-SCUBE3	Abnova	H00222663-A01
Anti-Smad1	Cell Signaling Technology	CST #9743
Anti-β-actin	Sigma-Aldrich	A5316
Alexa Fluor 488 Phalloidin	Cell Signaling Technology	8878
Goat anti-Mouse Alexa Fluor 594	Thermo Fisher Scientific	A-11020
Bacterial and Virus Strains		
DH5α	Yeastern Biotech Co., Ltd	#FYE607-8VL
Lentiviral	pSIN-MCS or pLKO.1 vector	
Chemicals, Peptides, and Recombinant Proteins		
Alcian blue	Sigma-Aldrich	A5268
Alizarin red S	Sigma-Aldrich	A5533
BMP2	R&D Systems	355-BM
BMP4	R&D Systems	314-BP
5-bromo-2'-deoxyuridine (BrdU)	Sigma-Aldrich	B9285
Calcein	Sigma-Aldrich	C0875
Collagenase D	Roche	11088858001
3,3'-diaminobenzidine (DAB) peroxidase	KPL	54-10-00
Eosin	Sigma-Aldrich	E4009
Entellan new	Merck	HX57317161
Hematoxylin	Sigma-Aldrich	H3136
Leukocyte (*TRAP*) *staining* kit	*Sigma*-Aldrich	*387A*
LumiFlash™ Femto Chemiluminescent substrate, HRP System	Visual Protein	LF24-100
Lipofectamine™ 3000	Life Technologies	L3000015
Noggin	R&D Systems	3344-NG
OptiPrep solution	Sigma-Aldrich	D1556
Orange G	Sigma-Aldrich	O3756
pGEM-T-Easy vector system	Promega	A1360
p-nitrophenol-phosphate	Sigma-Aldrich	N1890

Phloxin B	Sigma-Aldrich	P4030
Polybrene	Sigma-Aldrich	TR-1003
Protein A-agarose	GE	17-0780-01
Proteinase K	Roche	3115887001
Sirius red	Sigma-Aldrich	365548
T-Pro LumiLong plus chemiluminescence	T-Pro Biotechnology	JT96-K004M
TRIzol	Life Technologies	15596026
Experimental Models: Cell Lines		
C3H/10T1/2	American Type Culture Collection	CCL-226
HEK-293T	American Type Culture Collection	CCL-11268
Saos-2	American Type Culture Collection	HTB-85
Experimental Models: Organisms/Strains		
Scube3$^{-/-}$ mice	UCDavis	049572-UCD
Oligonucleotides		
Gapdh forward primer (5'-3') ATCATCCCTGCATCCACTGGTGCTG	Lin et al., 2015	RT-PCR
Gapdh reverse primer (5'-3') TGATGGCATTCAAGAGAGTAGGGAG	Lin et al., 2015	RT-PCR
Scube1 forward primer (5'-3') CGGCGGCGAACTTGGTGACTACA	Lin et al., 2015	RT-PCR
Scube1 reverse primer (5'-3') TTGATAAAGGACCGGGGGAACAT	Lin et al., 2015	RT-PCR
Scube2 forward primer (5'-3') TGACTACCTGGTGATGCGGAAAAC	Lin et al., 2015	RT-PCR
Scube2 reverse primer (5'-3') CAGTGGCGTGTGGGAAGAGTCA	Lin et al., 2015	RT-PCR
Scube3 forward primer (5'-3') TGCTCCCCGGGCCACTACTAT	Lin et al., 2015	RT-PCR
Scube3 reverse primer (5'-3') AGCGCTGTTGGCCTCACTGGTCTT	Lin et al., 2015	RT-PCR
Acvr1 forward primer (5'-3') CATCGCTTCAGACATGACCTC	Tsuji et al., 2006	Q-PCR
Acvr1 reverse primer (5'-3') CTAACCGTATCCAGAGTAGTG	Tsuji et al., 2006	Q-PCR
Acvr2a forward primer (5'-3') GTTGAACCTTGCTATGGTGATAA	Tsuji et al., 2006	Q-PCR
Acvr2a reverse primer (5'-3') AATCAGTCCTGTCATAGCAGTTG	Tsuji et al., 2006	Q-PCR
Alpl forward primer (5'-3') AACCCAGACACAAGCATTCC	Lin et al., 2015	Q-PCR
Alpl reverse primer (5'-3') GAGACATTTTCCCGTTCACC	Lin et al., 2015	Q-PCR
Bmp2 forward primer (5'-3') TGGAAGTGGCCCATTTAGAG	Tsuji et al., 2006	Q-PCR
Bmp2 reverse primer (5'-3') TGACGCTTTTCTCGTTTGTG	Tsuji et al., 2006	Q-PCR

Bmp4 forward primer (5’-3’) ACGTAGTCCCAAGCATCACC	Tsuji et al., 2006	Q-PCR
Bmp4 reverse primer (5’-3’) TCAGTTCAGTGGGGACACAA	Tsuji et al., 2006	Q-PCR
Bmp7 forward primer (5’-3’) TACGTCAGCTTCCGAGACCT	Tsuji et al., 2006	Q-PCR
Bmp7 reverse primer (5’-3’) GGTGGCGTTCATGTAGGAGT	Tsuji et al., 2006	Q-PCR
Bmpr1a forward primer (5’-3’) CCTGTTGTTATAGGTCCGTTCT	Tsuji et al., 2006	Q-PCR
Bmpr1a reverse primer (5’-3’) AGCTGGAGAAGATGATCATAGCA	Tsuji et al., 2006	Q-PCR
Bmpr1b forward primer (5’-3’) GGAAGACTCAGTCAATATCTGC	Tsuji et al., 2006	Q-PCR
Bmpr1b reverse primer (5’-3’) CTAGTCCTAGACATCCAGAGGTGAC	Tsuji et al., 2006	Q-PCR
Bmpr2 forward primer (5’-3’) AGCTGACAGAAGAAGACTTGGAG	Tsuji et al., 2006	Q-PCR
Bmpr2 reverse primer (5’-3’) CAAGCTAGAACTGGTACTGCTCA	Tsuji et al., 2006	Q-PCR
Col1a1 forward primer (5’-3’) ACGTCCTGGTGAAGTTGGTC	Lin et al., 2015	Q-PCR
Col1a1 reverse primer (5’-3’) CAGGGAAGCCTCTTTCTCCT	Lin et al., 2015	Q-PCR
Gapdh forward primer (5’-3’) CCAGAACATCATCCCTGCATC	Lin et al., 2015	Q-PCR
Gapdh reverse primer (5’-3’) CCTGCTTCACCACCTTCTTGA	Lin et al., 2015	Q-PCR
Ibsp forward primer (5’-3’) AAGCAGCACCGTTGAGTATGG	Lin et al., 2015	Q-PCR
Ibsp reverse primer (5’-3’) CCTTGTAGTAGCTGTATTCGTCCTC	Lin et al., 2015	Q-PCR
Ostcn forward primer (5’-3’) TGACAAAGCCTTCATGTCCA	Lin et al., 2015	Q-PCR
Ostcn reverse primer (5’-3’) TGCCAGAGTTTGGCTTTAGG	Lin et al., 2015	Q-PCR
Osterix forward primer (5’-3’) AGCGACCACTTGAGCAAACAT	This paper	Q-PCR
Osterix reverse primer (5’-3’) GCGGCTGATTGGCTTCTTCT	This paper	Q-PCR
Runx2 forward primer (5’-3’) GCAGTTCCCAAGCATTTCAT	Lin *et al*., 2015	Q-PCR
Runx2 reverse primer (5’-3’) GAAGGGTCCACTCTGGCTTT	Lin *et al*., 2015	Q-PCR
Sp7 forward primer (5’-3’) AGCGACCACTTGAGCAAACAT	This paper	Q-PCR

Sp7 reverse primer (5'-3') GCGGCTGATTGGCTTCTTCT	This paper	Q-PCR
Recombinant DNA		
pLKO.1	Addgene	#10878
pCMV-ΔR8.91	National RNAi Core Facility at	
pMD.G	National RNAi Core Facility at	
pFLAG-CMV1	Sigma-Aldrich	**E7273**
pSecTag2-HygroB	Thermo Fisher Scientific	V91020
pcDNA3.1	Thermo Fisher Scientific	V79020
pEGFP-C2	Addgene	#6083-1
Software and Algorithms		
ImageJ	https://imagej.nih.gov/ij/	
Prism 7	GraphPad Software	
SigmaPlot10.0	https://www.systat.com/	Serial #775066493

References

Kuczmarski, R.J., Ogden, C.L., Guo, S.S., et al. (2002) 2000 CDC growth charts for the United States: Methods and development. Data From the National Health Examination Surveys and the National Health and Nutrition Examination. Surveys Vital Health Stat 11(246). National Center for Health Statistics, Hyattsville, Maryland. DHHS Publication No. (PHS) 2002-1696.

Lin, Y.C., Roffler, S.R., Yan, Y.T., and Yang, R.B. (2015). Disruption of Scube2 Impairs Endochondral Bone Formation. J. Bone Miner. Res. *30*, 1255-1267.

Tsuji, K., Bandyopadhyay, A., Harfe, B.D., Cox, K., Kakar, S., Gerstenfeld, L., Einhorn, T., Tabin, C.J., and Rosen, V. (2006). BMP2 activity, although dispensable for bone formation, is required for the initiation of fracture healing. Nat. Genet. *38*, 1424-1429.

Appendix: The Genomics England Research Consortium

Ambrose J. C.[1], Arumugam P.[1], Baple E. L.[1], Bleda M.[1], Boardman-Pretty F.[1,2], Boissiere J. M.[1], Boustred C. R.[1], Brittain H.[1], Caulfield M. J.[1,2], Chan G. C.[1], Craig C. E. H.[1], Daugherty L.C.[1], de Burca A.[1], Devereau, A.[1], Elgar G.[1,2], Foulger R. E.[1], Fowler T.[1], Furió-Tarí P.[1], Hackett J. M.[1], Halai D.[1], Hamblin A.[1], Henderson S.[1,2], Holman J. E.[1], Hubbard T. J. P.[1], Ibáñez K.[1,2], Jackson R.[1], Jones L. J.[1,2], Kasperaviciute D.[1,2], Kayikci M.[1], Lahnstein L.[1], Lawson K.[1], Leigh S. E. A.[1], Leong I. U. S.[1], Lopez F. J.[1], Maleady-Crowe F.[1], Mason J.[1], McDonagh E.M.[1,2], Moutsianas L.[1,2], Mueller M.[1,2], Murugaesu N.[1], Need A. C.[1,2], Odhams C. A.[1], Patch C.[1,2], Perez-Gil D.[1], Polychronopoulos D.[1], Pullinger J.[1], Rahim T.[1], Rendon A.[1], Riesgo-Ferreiro P.[1], Rogers T.[1], Ryten M.[1], Savage K.[1], Sawant K.[1], Scott R. H.[1], Siddiq A.[1], Sieghart A.[1], Smedley D.[1,2], Smith K. R.[1,2], Sosinsky A.[1,2], Spooner W.[1], Stevens H. E.[1], Stuckey A.[1], Sultana R.[1], Thomas E. R. A.[1,2], Thompson S. R.[1], Tregidgo C.[1], Tucci A.[1,2], Walsh E.[1], Watters, S. A.[1], Welland M. J.[1], Williams E.[1], Witkowska K.[1,2], Wood S. M.[1,2], Zarowiecki M.[1]

1. Genomics England, London, UK
2. William Harvey Research Institute, Queen Mary University of London, London, EC1M 6BQ, UK.